CHALMERS

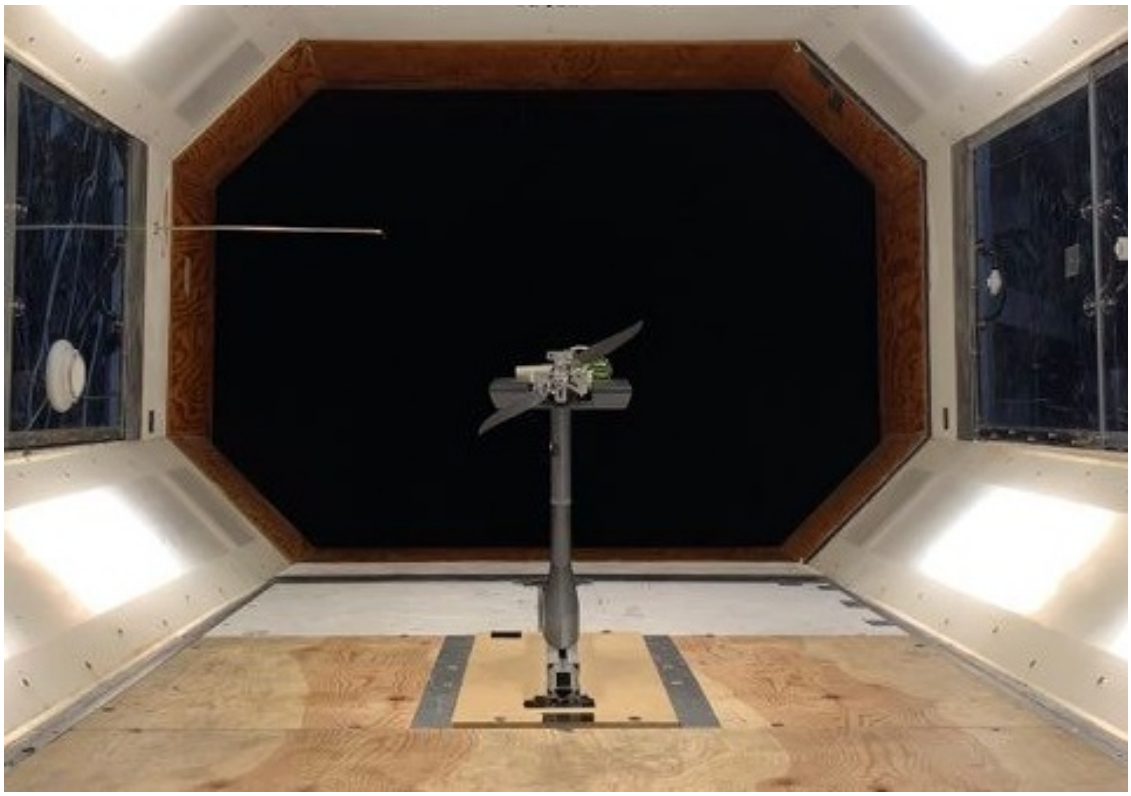

Propulsive Integration on a Search and Rescue Drone Aircraft

MMSX20-22-09

Authors:

Yasser Alrifai

Hayk-David Avetian

Carl Ingemarsson

Oliver Kadi

Victor Mathiesen

Maria Vassilev

Mechanical Engineering - Dept. of Mechanics and Maritime Sciences

CHALMERS UNIVERSITY OF TECHNOLOGY

Gothenburg, Sweden 2022

www.chalmers.se

Bachelor's Thesis 2022

Propulsive Integration on a Search and Rescue Drone Aircraft

CHALMERS

Department of Mechanics and Maritime Sciences
Division of Mechanical Engineering
Chalmers University of Technology
Gothenburg, Sweden 2022

Propulsive Integration on a Search and Rescue Drone Aircraft
YASSER ALRIFAI
HAYK-DAVID AVETIAN
CARL INGEMARSSON
OLIVER KADI
VICTOR MATHIESEN
MARIA VASSILEV

Supervisor: Isak Jonsson, Mechanics and Maritime Sciences
Examiner: Carlos Xisto, Mechanics and Maritime Sciences

Bachelor's Thesis 2022
Department of Mechanics and Maritime Sciences
Chalmers University of Technology
SE-412 96 Gothenburg
Telephone +46 31-772 10 00

Cover: Assembled testing rig inside a wind tunnel.

Typeset in LaTeX
Gothenburg, Sweden 2022

Propulsive Integration on a Search and Rescue Drone Aircraft
YASSER ALRIFAI
HAYK-DAVID AVETIAN
CARL INGEMARSSON
OLIVER KADI
VICTOR MATHIESEN
MARIA VASSILEV
Department of Mechanics and Maritime Sciences
Chalmers University of Technology

Abstract

The propulsive system is an integral part of any aerial vehicle because it is responsible for producing thrust, which in turn is what allows the vehicle to move through the air. This project investigates and implements a propulsive system to a search and rescue drone aircraft by developing a selection and combination of propellers and motors that will best serve for a given mission. The process for selecting motors and propellers is done by comparing existing products on the market with each other and examining their torque- and efficiency matching. Only a few of the top candidates are selected for further investigation with a testing rig in a wind tunnel, which in turn results in a few suitable combinations of motors and propellers for the dedicated mission and aerodynamic loads. From these results suggestions are made for how the propellers can be modified for a better fit for this specific application. Interesting follow-up projects could include further research by developing new propellers specifically for the application. Additionally, interesting follow-up projects could include further investigation of what kind of motor is optimal, and what batteries can be used and implemented into the drone aircraft.

Keywords: UAV, Propeller, Motor, Thrust, Torque, Efficiency, Propeller-Motor matching, Energy consumption

Acknowledgements

First and foremost we would like to extend a great thanks to our supervisor Isak Jonsson who helped us tremendously in successfully completing this project. His guidance, advice, and efforts have been invaluable to us. We have much appreciated his genuine interest to share his knowledge and expertise, as well as all the time spent on assisting us in completing the project.

We would also like to thank Edward Hadziavdic, for his help, care, and kind support to us. He made the Chalmers wind tunnel lab feel like a very friendly and welcoming place.

Finally, we would like to thank Petter Miltén and Christian Svensson for providing valuable help and knowledge. We would also like to extend our gratitude to our examiner Carlos Xisto for his efforts and expert advice.

Thank you all!

Yasser Alrifai
Hayk-David Avetian
Carl Ingemarsson
Oliver Kadi
Victor Mathiesen
Maria Vassilev
Gothenburg, May 2022

List of Acronyms

Below is the list of acronyms that have been used throughout this thesis listed in alphabetical order:

AoA	Angle of Attack
BDC	Brushed Direct Current
BLDC	Brush-Less Direct Current
BWB	Blended Wing Body
CAD	Computer Aided Design
CFD	Computational Fluid Dynamics
ESC	Electronic Speed Control
FEM	Finite Element Method
GPS	Global Positioning System
PSU	Power Supply Unit
rpm	revolutions per minute
SSRS	Swedish Sea Rescue Society
UAV	Unmanned Aerial Vehicle

Nomenclature

Below is the nomenclature of coefficients and parameters that have been used throughout this thesis.

Propeller Coefficients and Parameters

A_{disk}	Area of actuator disk
B_p	Number of propeller blades
C_P	Power coefficient
C_Q	Torque coefficient
C_T	Thrust coefficient
c	Chord
c_d	Drag coefficient
c_l	Lift coefficient
D	Drag
D_p	Propeller diameter
d_h	Propeller hub diameter
HTR	Hub to tip ratio
J	Advance ratio
J_{opt}	Optimum advance ratio
L	Lift
n	Angular velocity
P	Propeller power
P_{av}	Available power
P_{br}	Shaft power
Q	Torque
R_h	Propeller hub diameter
R_p	Propeller blade radius

r	Cross section radius
T	Thrust
V	Air speed velocity
V_{res}	Resulting speed of V_{rot} and V
V_{rot}	Cross section rotational speed
α	Blade angle of attack
α_{opt}	Optimum angle of attack
β	Blade pitch angle
$\eta_{propeller}$	Propeller efficiency
η_{turbo}	Turbo-efficiency
$\eta_{propulsive}$	Propulsive efficiency
ρ	Air density
ϕ	Blade advance angle
Ω	Peripheral velocity

UAV Coefficients and Parameters

D	Drag
c_d	Drag coefficient
c_l	Lift coefficient
L	Lift
q	Dynamic pressure
S	Reference area
T	Thrust
W	Self weight
α	UAV angle of attack
ρ	Air density

Motor Coefficients and Parameters

C_P	Power coefficient
C_Q	Torque coefficient
D_p	Propeller diameter
i	Current input into motor
$i_{m,max}$	Maximum allowed current

i_0	No-load current
K_v	No-load motor constant
n	Angular velocity
P_{el}	Electric power
P_m	Motor power
$P_{m,max}$	Maximum allowed power
P_{shaft}	Shaft power
Q_{prop}	Propeller torque
Q_m	Motor torque
v	Voltage input into motor
v_0	No-load voltage
η_m	Motor efficiency
ρ	Air density

Contents

List of Figures

List of Tables

1
Introduction

A drone, also known as an *Unmanned Aerial Vehicle* (UAV), is an aircraft without an on-board pilot, which means that it can be either remotely controlled or it can fly autonomously [1]. These types of aircraft were originally developed for military use such as the UAV 02 Falken, which was used for surveillance and can be seen in Fig. 1, but today they are used for more and more civilian applications.

UAVs have been especially useful for surveillance due to their long range, small size and cheap maintenance [3]. As a result it also allows them to operate in tough conditions and territories.

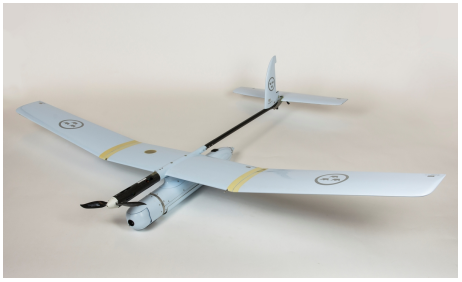

Fig. 1. UAV 02 Falken, an example of a military application of a drone. From [2].

As the progress in aeronautical engineering continues, the aim is to increase aircraft efficiencies even further by developing *Blended Wing Body* (BWB) aircrafts [4]. These aircrafts differ from conventional ones as the whole body of the aircraft resembles one flying wing. It is a design that improves fuel economy and efficiency because the entire BWB aircraft body produces lift, instead of just the wings. An illustration of this is shown in Fig. 2, where the X-48B BWB research aircraft is shown and its whole body resembles that of a wing.

With military technology development constantly improving and becoming more widely used it is eventually being brought to the commercial sector, similar to the *Global Positioning System* (GPS) [6]. The concept of a UAV could be argued to be in that phase, going from surveillance and carrying military ordnance to "everyday tasks like fertilizing crop fields on an automated basis, monitoring traffic incidents, surveying hard-to-reach places, or even delivering pizzas" [7].

1.1 Purpose

The Mechanics and Maritime Sciences department at Chalmers in collaboration with the *Swedish Sea Rescue Society* (SSRS) aims to use a blended wing UAV for offshore emergency search and rescue missions. A drone with a long range of operations will

greatly improve the chances of successful rescues and improve safety at seas. One important aspect of the development is the propulsive systems on the aircraft. Selection and combination of propellers and motors can greatly affect operational range, and therefore it is a vital aspect of the UAV design.

Fig. 2. The X-48B Blended Wing Body research aircraft. From [5].

The project is initialized by completing a screening to satisfy mission demands of the available motors and propellers on the market. These are then assessed and ranked in order to find the best performing candidates, in regards of energy consumption, for further testing. To further test the candidates, a testing rig must be acquired. For this to yield the best results it should also be redesigned to match the drone's shape. The candidates will later be tested in the wind tunnel available at Chalmers campus, to further evaluate the propulsive performance. The results should indicate the highest performing propeller and motor combination in terms of energy consumption, which is the main objective of the project.

1.2 Objectives

The objectives in this project can be summarized in the list below:

- Define the thrust requirement of the drone for all flight modes in a mission.
- Identify propellers suitable to the UAV and its mission.
- Identify a motor suitable for the the propeller while taking the drone flight conditions and constraints into account, as well as other criteria including weight, torque matching, power ratio, and current ratio.
- Redesign the acquired testing rig to match the drone's shape and characteristics.
- Identify the combination of motor and propeller available on market that together have the least possible power consumption per sortie while also taking into account that the weight of the drone may change.
- Identify a propulsive configuration that allows for accelerated takeoff.
- Identify each propulsive components' energy consumption as well as their energy consumption for an entire mission.
- Define what factors influence the propeller, motor, and overall UAV efficiency.

To summarize this project aims to develop and compare several propulsive configurations to find the overall best efficiency, in terms of energy consumption, of a search and rescue drone. While also taking into consideration the effects it has on the drone's maneuvering capabilities during take-off and flight.

1.3 Scope

This project is limited due to several factors, which are presented in 1.3.2 . The work on the propulsive system of the drone revolves around its mission and specifications. Therefore several delimiting factors should be taken into account.

1.3.1 Drone Mission

The drone mission is defined by the following points:

- At takeoff the drone will be given an initial airspeed of 10-15 m/s using a catapult. Time spent at takeoff is unknown, but an initial guess is 30 seconds at 15 m/s.
- The drone should reach its target within 20 minutes of flight. This flight mode is called sprint and is estimated to run at 35 m/s. As an estimation the time spent will be set to 20 minutes.
- When the drone has reached its target it will loiter at 20 to 25 m/s for 40 minutes. As an estimation the drone is set to fly in loiter at 22 m/s for 40 minutes.
- The drone is estimated to weigh 2.5 kg, however this number could change.
- The drone's angle of attack limit is set to 10°, to prevent stalling.
- The reference area of the drone is 2.97 dm^2

1.3.2 Delimitations

The project takes place during the time period for the Bachelor thesis provided by the Chalmers administration. This period ranges from the 18^{th} of January 2022 to the 12^{th} of May 2022. Time constraints as these limits the project and the possible outcomes.

All tests and measurements of the propeller and motor are done using existing facilities provided by Chalmers University of Technology in Gothenburg, Sweden. A larger test rig can be acquired if it is deemed necessary. Essentially all tests are made in a controlled environment which can limit the final results. This is also worth considering later on while discussing the results of the project.

Propellers and motors are purchased, since the aim of the project does not include the design of completely new components, but rather to select and integrate existing propellers and motors. The same goes for the design changes to the aircraft body.

There are no major changes, except for the eventual changes of the mounting area for the motor and propeller.

There are no *Computational Fluid Dynamics* (CFD) simulations on the propellers because of time constrains. As for any advanced deformation simulations, such as using the *Finite Element Method* (FEM) to calculate the deformation on the propeller blades, they are not included in the project as this is deemed outside of the scope.

2

Theory

This chapter presents the theory for understanding how propellers and motors work and how they interact with each other in order to find a combination with the lowest possible power consumption. This chapter also presents theory regarding the testing rig together with the included software and how it measures motor and propeller performance, as well as information regarding the wind tunnel. The aerodynamic terms necessary to fit the propeller and motor to the UAV are also introduced.

2.1 Basic Propeller Principles

Understanding how propellers work and how their performance is measured is an essential part of this project as they are responsible for pushing the drone through the air. This section presents the geometry of a propeller and the theory behind the generation of thrust, power and torque.

2.1.1 Geometry

A propeller can be represented as a set of airfoils, rotating around a hub. Each propeller blade has a chord, which is the center-line of the airfoil [8]. Due to rotation, cross sections closer to the hub have slower speed in the rotational plane, denoted V_{rot}. Further out towards the tip, V_{rot} becomes greater. The propeller moves forward in the air with an air speed velocity denoted V, which is the same for all cross sections of the propeller blade. For each cross section, the two velocities V_{rot} and V combined create V_{res}, that represents the resulting speed of the airflow hitting the blade, which varies along the blade.

Taking into consideration that velocity is a vector quantity, a set of angles can be defined between V_{res}, the chord, and the plane of rotation. The advance angle, denoted ϕ, is the angle between V_{res} and the plane of rotation, and the angle between V_{res} and the chord of the airfoil is called the angle of attack, denoted α. Summing the angles ϕ and α results in the angle between the chord and the plane of rotation. This angle is called the blade pitch and is denoted β [8]. An illustration of these angles can be seen in Fig. 3.

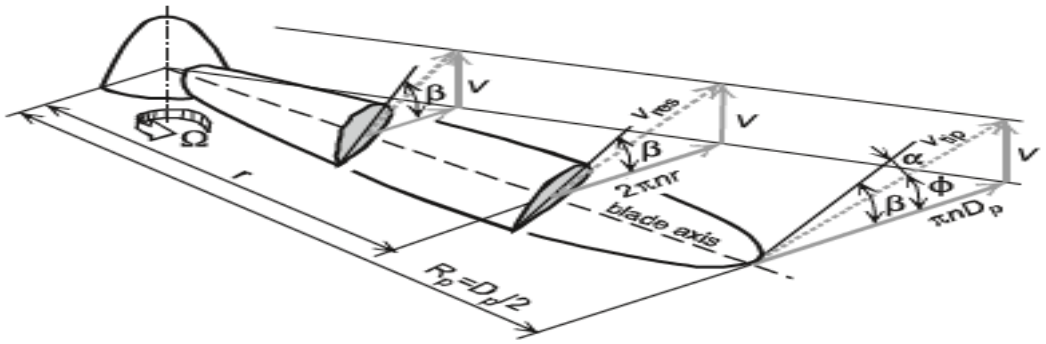

Fig. 3. Figure of a propeller blade. From [8]. Reproduced with permission.

Here R_p denotes the radius of the propeller blade and D_p denotes the diameter. The propeller size is usually given as diameter times pitch, and the pitch denotes the distance the propeller travels in the air after one revolution, similar to the thread of a screw.

Usually in any propeller there is an optimum angle of attack, denoted α_{opt}, which should be maintained in all propeller cross sections. If α is too large for any given cross section the airfoil will be stalled, meaning that the propeller is not moving any air back. If it is too small it does not produce any lift. Since the advance angle ϕ varies along the blade, in order to maintain α_{opt}, the blade pitch β is reduced for larger radii, denoted r. This results in a twist of the blade, as can be seen in Fig. 3. Each cross section closer to the tip of the blade has a reduced blade pitch angle β.

2.1.2 Blade-Element Theory

The *blade-element theory* expands the theory covered by taking the geometry into consideration and then determines the aerodynamic forces by splitting up the propeller blade into several smaller elements and calculating the forces on the elements [8]. By doing this, the characteristics of the propeller such as thrust, torque, advance ratio, and power coefficients can be decided [9].

As was first shown in Fig. 3, the propeller rotates around the hub with a peripheral velocity of Ω. Its peripheral velocity at the radius r and angular velocity n is

$$\Omega r = 2\pi n r \ . \tag{1}$$

This equation can then be used to calculate the resultant of the air speed velocity V as

$$V_{res} = \sqrt{V^2 + (\Omega r)^2} = V\sqrt{1 + (\pi/J)^2 \, (r/R_p)^2} \ , \tag{2}$$

where the *advance ratio* is defined as

$$J \hat{=} \frac{V}{nD_p} = \frac{V}{2n\,R_p}\ , \tag{3}$$

which is the ratio between the ambient air speed and the propeller diameter multiplied with the angular velocity [8].

For a small cross sectional element of the blade with chord c between r and (r + dr), as is shown in Fig. 4, the lift dL is perpendicular to V_{res}.

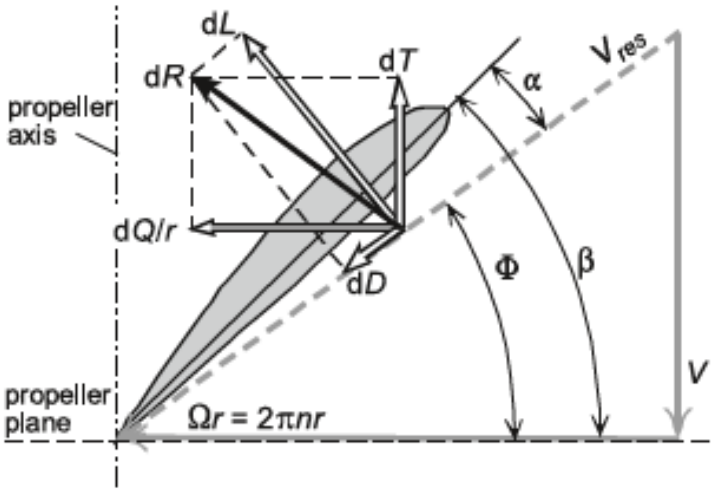

Fig. 4. Small cross sectional element of a blade. From [8]. Reproduced with permission.

The drag dD is parallel to V_{res}, and the air force dR is the sum of dL and dD [8]. Using dR, the thrust component dT and the torque component dQ/r can be found by projecting the vectors in the V, respectively the V_{rot} planes,

$$dT = dL\,cos\,\phi - dD\,sin\,\phi \qquad \text{and} \qquad dQ/r = dL\,sin\,\phi + dD\,cos\,\phi\ . \tag{4}$$

The blade thrust is obtained by the following integration over all elements along the radius of the blade

$$T = B_p \int_{R_h}^{R_p} (c_l\,cos\,\phi - c_d\,sin\,\phi)\,\frac{1}{2}\,\rho\,V_{res}^2\,c\,\mathrm{d}r\ , \tag{5}$$

where c_l and c_d are the lift and drag coefficients, both determined by the local angle of attack α, and ρ is the air density [8]. R_h here denotes the propeller hub diameter, and for simplification, it is assumed to be zero. By multiplying with the number of blades, B_p, the total propeller thrust can be calculated. The thrust coefficient is defined as

$$C_T \hat{=} \frac{T}{\rho\,n^2\,D_p^4}\ . \tag{6}$$

In a similar way, the propeller power is found by integrating the torque over the blade. The power coefficient is defined as

$$C_P \hat{=} \frac{P}{\rho\, n^3\, D_p^5}\ . \tag{7}$$

By inserting (2) into (5) and evaluating both the thrust coefficient C_T and the power coefficient C_P, it can be shown that they are only dependent on the blade pitch angle β and the advance ratio J [8].

The torque of the propeller is found by integrating the blade element torque over the entire blade. The torque coefficient of the propeller is defined as

$$C_Q \hat{=} \frac{Q}{\rho n^2 D_p^5}\ . \tag{8}$$

2.1.3 Propeller Efficiency

One way to measure the performance of a propeller is to consider the propeller efficiency [8]. This is used to compare the power supplied to the propeller and its output power. It is defined as

$$\eta_{propeller} \hat{=} \frac{P_{av}}{P_{br}} = \frac{T\,V}{P_{br}}\ , \tag{9}$$

where P_{br} is the shaft power supplied by the motor, and P_{av} is the available power. For steady flight the shaft power P_{br} is equal to the propeller power P. T and P are replaced with C_T and C_P using (6) and (7). The efficiency can then be rewritten as

$$\eta_{propeller} = \frac{C_T}{C_P} J\ . \tag{10}$$

Note that if the aircraft velocity is zero, the advance ratio is also subsequently zero. This means that if the aircraft is stationary, the efficiency becomes zero.

In Fig. 5, the propeller efficiency $\eta_{propeller}$ is plotted against the advance ratio J for a constant blade pitch.

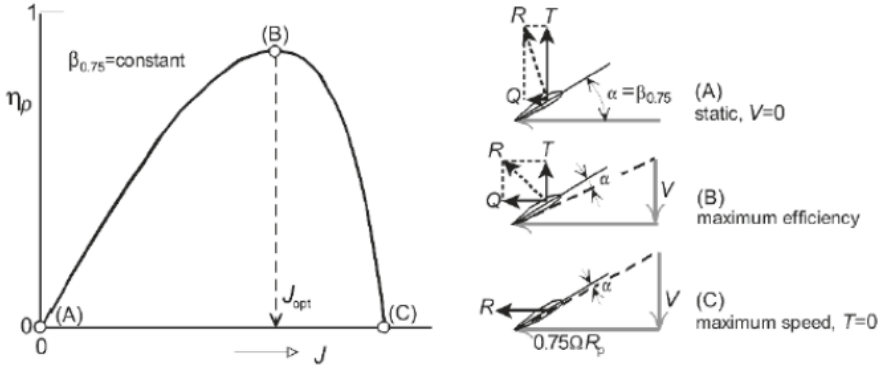

Fig. 5. Propeller efficiency and advance ratio for various flight speeds. From [8]. Reproduced with permission.

As presented in (3), J is the ratio between air speed V and blade diameter D_p multiplied with the angular velocity n. For low air speeds the thrust is large but the propeller is inefficient due to the low velocity, leading to a low output power compared to the supplied engine power. At high speeds the torque is large, but the thrust becomes close to zero due to force of the air shifting direction due to more drag. Therefore the efficiency is also near zero.

The efficiency peak can be shifted towards higher or lower advance ratios as shown in Fig. 6, by changing the blade pitch. Between the low and high air speeds there exists an optimum air speed, with an advance ratio J_{opt}, visualised in Fig. 5. This figure is achieved by tweaking the angular velocity or the propeller diameter at constant air speed for a generic propeller.

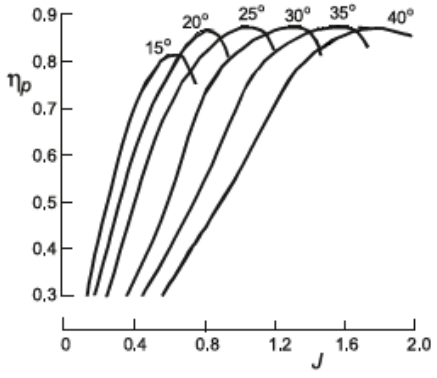

Fig. 6. Propeller efficiency vs. advance ratio for various blade pitches. From [8]. Reproduced with permission.

At constant air speed and angular velocity, a large diameter will result in a low J, and the propeller has a risk of stalling. The opposite occurs with small diameters, J becomes large and results in a thrust that is close to zero, a large torque, and a low propeller efficiency. The same results can be seen in the case where the air speed and propeller diameter is constant; a high angular velocity results in a low J, and a low angular velocity results in a high J.

2.1.4 Actuator Disc Theory

The *Actuator Disk Theory* [10] is used to derive some important efficiency quantities for propellers. This theory idealizes and simplifies the propeller by replacing it with a disk with an infinitesimal thickness. In addition to this few assumptions are made:

1. The air flow is not affected by the rotation.
2. The air speed velocity is low so that the flow acts as an in-compressible fluid.
3. No work is put on the flow outside the disk stream-tube.
4. The flow is steady state.
5. The pressure change over the disk is not continuous, but the velocity change is.

2.1.5 Propulsive efficiency

In section 2.1.3 propeller efficiency was introduced. This physical quantity measures how much of the energy that the propeller uses for its thrust. In this section propulsive efficiency will be examined. It is a physical quantity that is more oriented to the energy of the propeller being converted to kinetic energy in the air leaving the propeller, instead of only thrust. It is more directed at measuring how much of the jet leaving the propeller is used to propel the aircraft forward, and how much air is moving unnecessarily [11]. This is an idealized measure of efficiency, in the sense that it compares the ideal minimum power that the propeller needs to operate to the thrust it produces. Other measures of efficiency for a propeller will for that reason usually be lower than the propulsive efficiency [10].

Using the actuator disc theory described in 2.1.4, expression for the propulsive efficiency becomes:

$$\eta_{propulsive} = \frac{2}{1 + \left(\frac{T}{A_{disk}\, V^2\, \frac{\rho}{2}} + 1 \right)^{\frac{1}{2}}} \quad , \tag{11}$$

where T is the thrust, A_{disk} is the area of the actuator disk, V is the flight velocity, and ρ is the air density. For a full derivation of this expression, see [10].

2.1.6 Turbo-Efficiency

Another measure of efficiency for propellers is the turbo-efficiency. It is similar to the propulsive efficiency in that it compares the power corresponding to the kinetic energy that the propeller produces from the shaft power. The difference is that it does not assume that the propeller generates the ideal amount of power. The turbo-efficiency measures how much of the shaft power that is used to actually propel the aircraft forward and compares the increase of the kinetic energy from the air passing the propeller to the power supplied from the shaft. The assumptions made

in actuator disc theory described in 2.1.4 are applied for the turbo-efficiency as well, except that the hub area is taken into account by being subtracted from the disc area.

The turbo-efficiency equation is derived by A.Lind. For full derivation see [12]. The resulting expression is

$$\eta_{turbo} = \frac{T}{2P}\left(\sqrt{\frac{2T}{\rho\frac{D_p^2\pi}{4}(1-HTR^2)} + V^2} + V\right), \tag{12}$$

where $HTR = d_h/D_p$, is the hub to tip ratio, and d_h is the hub diameter of the propeller hub.

2.1.7 Force Equilibrium

The flying aircraft can be assumed to be in force equilibrium. As the aircraft flies, the forces acting on it are lift, drag, propeller thrust, and the drone weight. The drag and lift vary due to air speed and angle of attack of the aircraft. As lift is correlated with drag, minimum drag is given by the minimum lift that the aircraft can provide at a certain angle of attack and air speed, thus the thrust is a function of those parameters. In order for the drone to maintain stable flight, the lift needs to counter the weight, and the propeller thrust needs to counter the projection of the forces in the propeller planes, see Fig. 7.

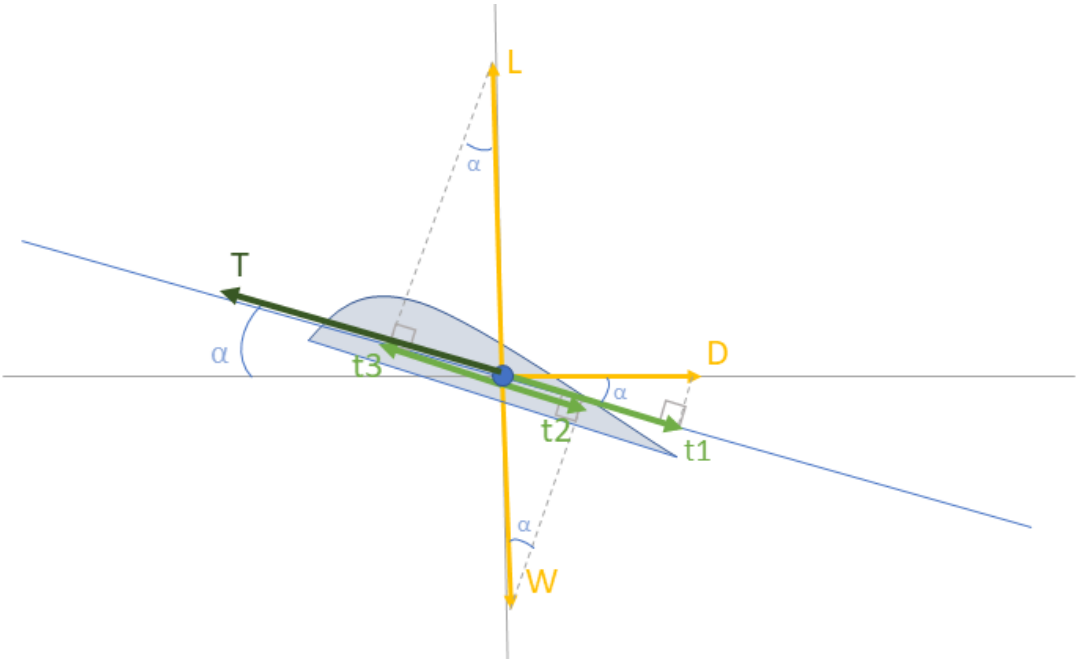

Fig. 7. Forces acting on a UAV in flight.

In Fig. 7 the drone flies with an angle of attack α and an air speed that induces lift L and drag D. The drone has a weight W. These forces act in the vertical and horizontal planes. In order to calculate the thrust, the propeller has to produce these forces projected on the chord plane. Doing a vertical force equilibrium in Fig. 7 the expression can be written as

$$L - W + T sin(\alpha) = 0 \; . \tag{13}$$

This means that in order to maintain stable flight the lift and vertical thrust component has to balance the weight.

The components along the chord line can be summed up as

$$T + t_3 - t_1 - t_2 = 0 \implies T = t_1 + t_2 - t_3 \; , \tag{14}$$

where t_1, t_2, and t_3 are the projections in the propeller plane of drag D, weight W and lift L respectively. With trigonometry the projections can be rewritten as

$$t_1 = D \, cos(\alpha) \; , \tag{15}$$

$$t_2 = W sin(\alpha) \; , \tag{16}$$

$$t_3 = L \, sin(\alpha) \; . \tag{17}$$

Inserting (15), (16), and (17) in (14) gives the result

$$T = D \, cos(\alpha) + W sin(\alpha) - L \, sin(\alpha) \; . \tag{18}$$

This is the minimum required thrust the propeller has to deliver in order for the drone to maintain stable flight.

The values for lift and drag can be calculated using the equations presented in a thesis written by Xisto et al. [13]. Here they are defined as

$$L = c_l \, q \, S \qquad and \qquad D = c_d \, q \, S, \tag{19}$$

where S is the reference area, c_l and c_d are lift and drag coefficients, and q is the dynamic pressure which is given by

$$q = \frac{\rho \, V^2}{2} \; , \tag{20}$$

where ρ is the air density, and V is the air velocity.

2.2 Electric DC Motor Principles

This section examines electric motors, which is a necessary part of the drone's propulsive system as they allow the propellers to rotate and lift the drone in the air. Electric motors use electromagnets to function, which themselves are made of coiled electrical wire which passes an electrical current to generate a magnetic field [14].

2.2.1 BLDC Motors

There are two types of commonly used electric direct current motors, *Brush-Less Direct Current* (BLDC) motors and *Brushed Direct Current* (BDC) motors, however BLDC is more beneficial for the drone for several reasons, including but not limited to; better efficiency as well as ability to reach higher speeds [15]. A typical BLDC motor can be seen in Fig. 8.

Fig. 8. One of the BLDC motors used in the project.

A BLDC motor has a certain amount of electromagnets, also known as magnetic poles. The number of poles will prove to be useful in the testing phase where this is an important parameter needed by the software used by the testing rig [16]. The number of rotations of the coil determines the resistance of the motor which sequentially determines the characteristics of the motor.

All motors have a specified no-load motor constant denoted K_v, a no-load current denoted i_0, and a no-load voltage denoted v_0. The no-load values in turn help determine the properties such as the maximum allowed current, $i_{m,max}$, and the maximum allowed power, $P_{m,max}$. It is important to note that the angular velocity, which also affects the motor constant, is usually given in the unit *revolutions per minute* (rpm), but for this section and its equations, the unit *radians per second* (rad/s) will be used.

In the context of designing a propulsive system for a drone, the motor torque, power, and efficiency have to be defined. A conservative method to calculate the motor torque can be expressed as [17]

$$Q_m = \frac{(i - i_0)}{K_v} \, , \tag{21}$$

where Q_m is motor torque, and i is the current input into the motor. The shaft power is the power output at the shaft of the motor and is defined as the product of motor torque and the angular velocity, which is expressed as [17]

$$P_{shaft} = Q_m \, n \, , \tag{22}$$

where n is the angular velocity. The electric power of any motor can be expressed as

$$P_{el} = v \cdot i \, , \tag{23}$$

where v and i are the voltage and current used. By dividing (22) with (23), an expression for the motor efficiency can be obtained as

$$\eta_m = \frac{P_{shaft}}{P_{el}} \, . \tag{24}$$

2.2.2 Motor-Propeller Matching

Motor-propeller matching is needed to assure that a relevant combination is chosen for the purpose of this project. It is a method that is based on the simple concept of matching the torque needed by a propeller and the torque produced by the motor as

$$Q_m = Q_{prop} \, . \tag{25}$$

Where Q_{prop} can be expressed as [18]

$$Q_{prop} = C_Q \, \rho \, n^2 D_p^5 \, , \tag{26}$$

and the torque coefficient C_Q can be expressed as

$$C_Q = \frac{C_P}{2\pi} \, . \tag{27}$$

2.2.3 ESC

The *Electronic Speed Control* (ESC) is another necessary part in the propulsive system of the drone. As the name suggests, it is a device that helps the drone regulate speed mid-flight. According to Unmanned System Technologies [19] "A signal from the flight controller causes the ESC to raise or lower the voltage to the motor as required, thus changing the speed of the propeller." By changing the voltage, the electrical power put into the motor will change, and subsequently change the angular velocity of the propeller.

2.3 Testing Rig

To measure the performance and characteristics of the motors and propellers, they have to be tested in a wind tunnel, using a testing rig. For this project a model *RCbenchmark Series 1580 Thrust Stand and Dynamometer* from Tyto Robotics was used. In addition to the hardware, it comes with a software program that automatically draws graphs with the measured values and calculates the efficiency of the electrical components. The last part of this section also presents how the shape of the testing rig body affects the air flow.

2.3.1 Measurement

In the testing rig measurements, two families of quantities are measured. The first type is electrical quantities, namely electrical potential and current. These values are measured directly by the software supplied by *TyTo robotics*.

Physical quantities is the second type and these are measured by loading cells inside the testing rig. Two loading cells are placed in the top horizontal plane of the testing rig, as can be seen in Fig. 9. These load cells measure torque by sensing the displacement of the surface in the sensor-rod material.

Fig. 9. Fully assembled testing rig with a motor and propeller in place.

Inside the vertical body of the testing rig is another loading cell, that measures the thrust generated from the motor and propeller by sensing the displacement in the sensor-rod caused by the thrust force.

2.3.2 Efficiencies

From the physical quantities of the motor that are measured by the testing rig, the efficiencies can be derived. There are three types of efficiencies that are used in the software, namely motor efficiency, propeller mechanical efficiency, and the overall efficiency. The motor efficiency is calculated as [16]

$$Motor\,Efficiency = \frac{Mechanical\,Power}{Electrical\,Power} = \frac{|Torque \times RotationSpeed|}{|Voltage \times Current|}\,, \quad (28)$$

which is used to determine if the motor and ESC are working well together.
The second efficiency, propeller mechanical efficiency, is calculated as [16]

$$Prop.\,Mech.\,Eff. = \frac{Thrust}{Mechanical\,Power} = \frac{Thrust}{|Torque \times RotationSpeed|}\,. \quad (29)$$

This efficiency is mainly used to determine the propeller performance, and how well it works with the motor.
Finally, the overall efficiency is calculated as [16]

$$Overall\,Efficiency = \frac{Thrust}{Electrial\,Power} = \frac{Thrust}{|Voltage \times Current|}\,, \quad (30)$$

and is used to evaluate if the propeller works well with the power chain, and the overall flight performance.

2.3.3 Pressure Drag over a Symmetric Airfoil

For a symmetric airfoil at zero degrees angle of attack, no lift will be generated. Since lift is primarily generated by the pressure differential over the airfoil, the lift will be equal to zero due to the symmetry.

The main type of drag over an object moving through a fluid is caused by pressure drag. Pressure drag is caused by the air molecules being compressed relative to the front-facing surface of the object, and decompressed relative to the surrounding air pressure in the free-stream behind the object.

The fluid flowing around the object generates a boundary layer on the surfaces, which when separated starts to swirl. This is known as turbulent flow.

Turbulent flow can be reduced to laminar flow, by making the object moving through the fluid more streamlined. Making an object more streamlined depends on many factors, but primarily boundary layer separation needs to be minimized. The coefficient of drag, c_d, gives a brief indication of how aerodynamic an object is when moving through a fluid at a certain speed [20]. The principle is shown in Fig. 10.

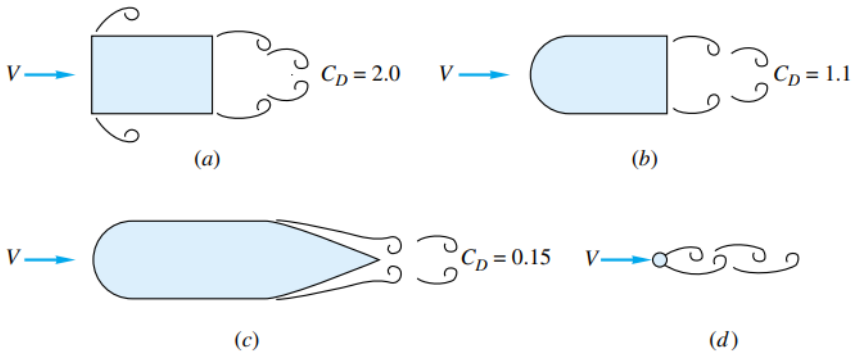

Fig. 10. The importance of streamlining in reducing drag of a body (c_d based on frontal area): (a) rectangular cylinder; (b) rounded nose; (c) rounded nose and streamlined sharp trailing edge; (d) circular cylinder with the same drag as case (c). From [20]. Reproduced with permission.

Skin friction is also a contributing factor to drag. When an object is moving through a fluid, the molecules closest to the surface will slow down, and right at the surface, the molecules will come to a complete stop. This is also known as the no-slip condition. Depending on the surface roughness, the regions in the boundary layer will look differently. Therefore, a slim surface with low roughness will not affect free stream as much as a surface with high roughness [20].

This theory is applied when designing the testing rig casing, in order to reduce the effect of drag on the measurements made by the rig.

2.4 Wind Tunnel

To be able to yield realistic measured data from the testing rig, an artificial wind must be added to avoid having static conditions. Data realistic to the mission is measured from propellers in an air flow, and to do this a wind tunnel is used. A wind tunnel is a confined area where an air flow is generated to simulate flight conditions [21]. In a wind tunnel, the environment can be controlled by adjusting the air flow conditions. By having a separate environment where the testing rig is placed, the environmental factors are also different, so they must be measured. The measured factors are temperature, air pressure, air flow speed, and air density.

3
Methods

In this chapter the methods for determining the best propeller and motor are presented. Here the initial screening methods for the propellers and motors are described. Furthermore, the wind tunnel testing procedures for both propellers and motors are also presented. In order to test the hardware in the wind tunnel, a rig has been constructed, the method of which is also described in this chapter.

3.1 Propeller Screening

In this section the propeller screening method will be described. In a database from UIUC Aerospace Group [18], propeller measurements for a variety of propeller brands, diameters and pitches are available. This data is used to do an initial screening of the propellers, in order to determine what propellers should be ordered to continue with further testing in the wind tunnel. The data is loaded from the database, and run in MATLAB to control that the propeller is able to deliver enough thrust. The propellers that pass this screening are run in a second MATLAB program in order to further investigate how the propellers perform in the conditions that are expected during a mission. The results from this second screening is used to rank the propellers, and finally conclude what propellers will progress to further testing.

3.1.1 Propeller Data and Measurements

The project uses data from a database that has been made by UIUC Applied Aerodynamics Group [18]. This database consists of three volumes of different propellers and measurements of propeller coefficients such as C_P, C_T, and $\eta_{propeller}$ for different angular velocities and advance ratios. With this data the performance of every propeller can be simulated, which will be presented later in the process.

3.1.2 Propulsive System Requirements

The requirements of the system is based on an aerodynamic model of the UAV. The lift and drag forces as well as their respective coefficients have been simulated in CFD, for multiple angles of attack and air speeds. This data is used together with (18) to find the minimum propeller thrust for the respective flight modes in

the drone mission.

3.1.3 Propeller Screening

In the process of selecting propellers an initial filtering was made on the large propeller database [18], selecting propellers that would perform satisfactory to accomplish the mission. The first requirement was to be able to generate enough thrust to maintain stable flight, and the second was that the simulated data points need to be in close proximity to the data curves given in the database. Propellers that pass this screening move on to the next step in the selection process.
A program was written in MATLAB for this process, and it does following operations in order:

1. Load propeller data from database $J, C_T, C_P, \eta_{propeller}$, and UAV-simulation data (velocities, angle of attack, drag, lift) for all flight modes.
2. Select an angle of attack in the simfile (2-4 °), that produces enough lift to balance the drone self-weight. For that lift find the corresponding drag.
3. Calculate minimum required thrust from UAV-simulation data for selected angle of attack, by inserting the lift and drag into (18).
4. Approximate three cubic piece-wise models of the loaded propeller data. J as independent variable, and $C_T, C_P, \eta_{propeller}$ respectively as dependent variables.
5. Make an initial guess of n. Calculate J from flight data and n using (3).
6. Call on the models of propeller constants using calculated J, and estimate $C_T, C_P, \eta_{propeller}$ for all flight modes.
7. Calculate propeller thrust from C_T using (6), and compare it to minimum thrust required by the UAV-simulation data for all flight modes. If the propeller produces more thrust than the minimum required in all flight modes it passes, otherwise it is rejected.
8. Estimate energy usage of all flight modes, using (7) to find power consumption and multiplying with total time spent in all flight modes.
9. Plot original data points from database into three different graphs, J on the x-axis and $C_T, C_P, \eta_{propeller}$ respectively on y-axis.
10. In same plots as the original propeller data, plot the approximations of C_T, C_P and $\eta_{propeller}$ from flight conditions.
11. Display results in command window, and if propeller is accepted or rejected.

    Since the angular velocity is guessed, a few different values of n were tried for each propeller in order to give each propeller a fair chance. In order to accept a propeller, the graphs had to look reasonable and the propeller also had to be able to deliver enough thrust for stable flight in all flight modes. Otherwise the propeller was rejected.

3.1.4 Downselection of Propellers

The ranking is done by writing a second program in MATLAB. Just as before the program calls for propeller and UAV data. But instead of having a fixed angular velocity, this code loops over different values in an interval of n. The code also runs for a set of different drone weights ranging between 2 and 4 kg. This is done as the final drone weight is currently unknown.
For each flight mode (takeoff, loiter, sprint) and drone weight the code do the following operations in order:

1. Load propeller data from database $J, C_T, C_P, \eta_{propeller}$, and UAV-simulation data (velocities, angle of attack, drag, lift) for all flight modes.
2. Approximate cubic piecewise model between lift and UAV angle of attack, as well as a model between drag and angle of attack.
3. For current drone weight, compute minimum required lift to balance drone self weight using (13), but disregard the thrust component, as it is currently unknown and has a negligible contribution to the lift requirement.
4. Using the model between lift and angle of attack, compute angle of attack requirement to maintain stable flight using the lift computed in previous step.
5. Using the model between drag and angle of attack, compute the drag associated with the angle of attack requirement.
6. Compute the minimum thrust requirement for current weight and flight mode using (18).
7. Create an interval of n, and loop n over the code.
8. Calculate J from flight data with (3), for the current n in the loop.
9. Call on the models of propeller coefficients using J in order to find C_T.
10. Calculate thrust T using (6). Compare to minimum required thrust to barely keep the drone in flight. If the estimated thrust is larger than the minimum allowed thrust, the program calculates power consumption with (7) and efficiency with (10). These values are then saved.
11. Once the program has looped over all flight modes, weights and angular velocities, it finds the lowest power consumption among the values saved in previous step for each flight mode and weight. It also selects the corresponding, $J, \eta_{propeller}$ and n.
12. The lowest power consumption in each mode is multiplied with the time spent in that mode and summed together with the energy consumption in the other modes. This is done in order to estimate the energy consumption for the sortie, which will later be used to rank the propellers.
13. C_P, C_T, and $\eta_{propeller}$ for each flight mode are plotted against J on top of the propeller database measurements.
14. The program outputs propeller power and energy consumption for each flight mode, optimal rpm, and total sortie energy consumption as well as other useful data.

From this program, the propellers were ranked according to their total energy consumption for all weights, since it was deemed the most crucial for the drone to accomplish its mission. The propeller with the lowest energy consumption is the highest ranking. The program also output graphs, if the graph looked off-centered the propeller was rejected.

The turbo- and propulsive efficiencies were determined separately. The propulsive efficiency was calculated by applying (11) to the thrust computed for all flight modes by the program described above.

The turbo-efficiency of the propellers in relation to the advance ratio was determined using the measurements from the UIUC database [18]. Since the angular velocity at which the measurements were made was known, the velocity of the air could be computed for every measured advance ratio using (3). For each measured J, the thrust and power were computed using (6) and (7). The computed power, thrust, and velocity were then input into (12) to compute the turbo-efficiency.

To find the turbo-efficiency specific to the flight modes, first a model between the turbo-efficiency and advance ratio was made. Then the advance ratios at which the drone operates (computed by the program described above) were put into the model to obtain the turbo-efficiency for each flight mode. The turbo-efficiency for all database measurements was then plotted against the advance ratio together with the turbo-efficiency for each flight mode.

3.1.5 Takeoff Capability

A program was written to compute the maximum forward acceleration the propeller can achieve but also how fast the UAV can climb. Simply put, the aim of the program is to estimate the maximum thrust and acceleration the propeller can achieve, regardless of motor performance. The program do the following operations in order:

1. Loads propeller measurements and UAV-simdata.
2. Set UAV angle of attack to 10°. Find corresponding c_l and c_d using mathematical models.
3. Compute lift and drag using (19).
4. Calculate upward net force by subtracting self weight from lift force. Upward acceleration is found by dividing upward net force with UAV mass.
5. Calculate minimum required propeller thrust using (18).
6. From the propeller data and take off velocity, find the lowest measured J. From J, calculate angular velocity using (3).
7. Find the corresponding C_T and C_P and calculate thrust and power using (6) and (7).
8. Calculate forward net force by subtracting minimum required thrust from propeller thrust. Find forward acceleration by dividing with UAV mass.

The program also outputs the following:

- UAV lift force for angle of attack 10°.
- Net upward force
- Upward acceleration
- Minimum required thrust for stable flight.
- Propeller thrust.
- Net forward force.
- Forward acceleration.
- Graphs plotting database measurements and takeoff point in data.

3.2 Motor Screening

This section describes the downselection of the motors with all included steps. This includes data collection and the ranking of motors.

3.2.1 Data Collection

In order to perform a motor screening the necessary data had to be collected. This data was found through cross-referencing a data-sheet found online [22] with the official data from the manufacturers website [23]. In this case the necessary data needed could be condensed to the following list of properties:

- Motor specific no-load K_v.
- Motor specific internal resistance
- Motor specific limiting factors such as:
  - Power
  - Current
- Motor specific physical attributes, such as:
  - Weight
  - Length and diameter

This information is often provided and does not require any further calculations. Once the motor characteristics were known the case specific data had to be collected. Case specific data can be defined as the specific data for a certain propeller at a certain flight mode that was derived by the methods used in section 3.1. This data includes:

- Operating angular velocity needed.
- Operating power consumption.

3.2.2 Motor Ranking

With the collected data, the specific requirements for each motor could be calculated. This includes the voltage, current, and torque required at takeoff, loiter, and

sprint, and are used to determine whether the motor characteristics are suitable for the requirements of the propeller. If the above mentioned motor values does not meet the minimum required values calculated from the propeller data, the motor is disregarded.

The non-viable motors were then discarded moving into the second screening process. This process assigned scores to the motors based on seven criteria:

1. Lowest torque difference percentage in loiter.
2. Lowest torque difference percentage in sprint.
3. Lowest current usage to maximum current ratio in loiter.
4. Lowest current usage to maximum current ratio in sprint.
5. Lowest power usage to maximum power ration in loiter.
6. Lowest power usage to maximum power ration in sprint.
7. Lowest motor weight.

The propeller-motor torque difference percentage is a value found through a method described in appendix B. A reference value of 35% was calculated by using this method with data from testing the unmodified testing rig with a combination of motor and propeller that was available. Every motor had their torque difference percentage calculated and compared to the reference value. If the torque difference for a motor was greater than the reference value, then it was discarded.

All the motors that made it through this stage of elimination were ranked in order of most appropriate to least. The five highest ranked were chosen for further testing and data validation.

3.3 Testing Rig

This section describes the methods used to redesign and rebuild the provided testing rig. It also describes the methods used for testing and verification of both thrust and torque sensors readings through a thorough calibration.

3.3.1 Redesign

The testing rig provided by Tyto Robotics is shown in Fig. 11. It was redesigned in order to make it more streamlined, and subsequently get more realistic results from the motor and propeller testing in the wind tunnel. A digital mock up of the initial new design was created in the *Computer Aided Design* (CAD) software Fusion 360. The new internal structure which holds the rig itself was then manufactured and assembled. In order to make the airflow around the rig streamlined, the bodies created in the digital mock up were manufactured using a 3D-printer and then assembled.

3.3.2 Sensor Testing

The testing rig has three sensor systems which measure the thrust, torque, and angular velocity, and the data is calibrated using *RCbenchmark Data-Acquisition Software* from Tyto Robotics. Calibration of the rig is done with a 200 g weight which is placed on certain places on the rig in specific order. To verify that the rig and software calibration gave correct values, more weights were used to ensure linear proportionality to load changes. The angular velocity was measured with a connection to one of the three motor power lines and was derived from the pulse modulation signals in the cable. The angular velocity could also be verified with a laser-sensor gun.

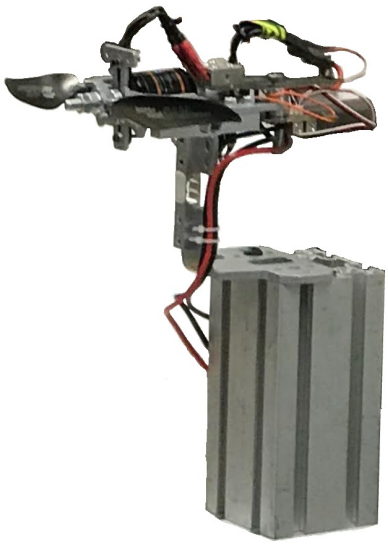

Fig. 11. Testing rig without any modifications.

The final design of the testing rig is presented in Fig. 9. The vertical airfoil directs the air around the rig and its sensors which ensures a smooth flow and more accurate results regarding the thrust readings. The airfoil in the horizontal plane creates an airflow similar to the the airflow across the drone itself. This airfoil also houses the circuit board, power cables, data cables and cables to the sensors.

3.3.3 Verification of Thrust Sensor Calibration

To ensure that the verification of thrust was successfully done, different weights ranging from 200 g to 1000 g were used. If the calibration was done correctly, then the weights would show the respective values shown in table I

TABLE I
THEORETICAL THRUST CALIBRATION VALUES

Weight [g]	**Thrust [N]**
200	1.962
400	3.924
600	5.886
800	7.848
1000	9.810

3.3.4 Verification of Torque Sensor Calibration

Following the same concept used in verifying the thrust sensors, different weights were placed on the end of the calibration plate to examine which values the sensors would provide. If the sensors were correctly calibrated, then the sensors would show the respective values seen in table II.

TABLE II
THEORETICAL TORQUE CALIBRATION VALUES

Weight [g]	**Torque [Nm]**
200	0.255
400	0.510
600	0.765
800	1.020
1000	1.275

3.3.5 Calibration Values

As can be seen in Fig. 12, the blue line describes the theoretical values that are expected and the red squares show the values that have been acquired from the manual calibration.

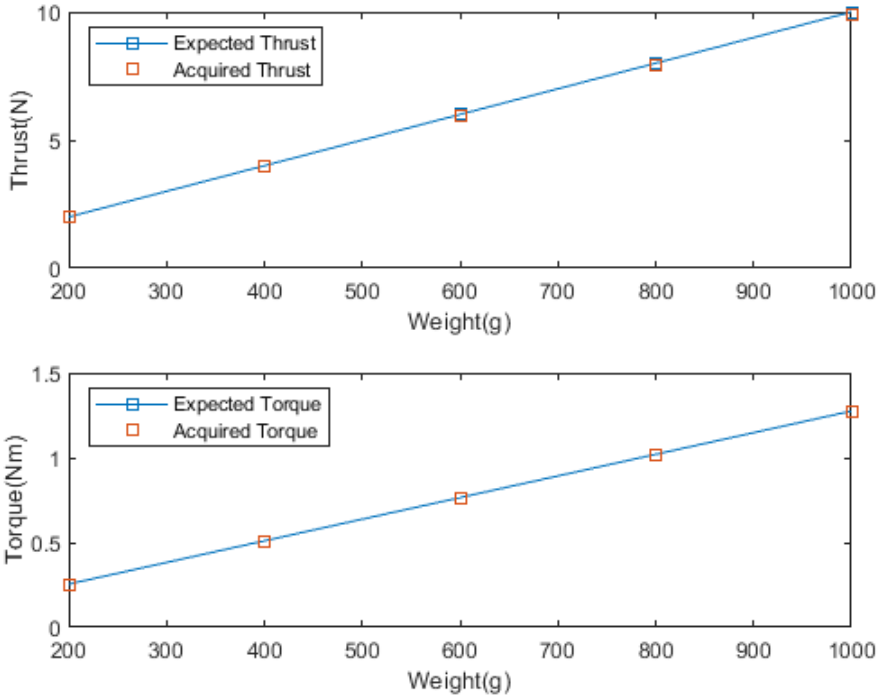

Fig. 12. Values from the manual calibration: expected values and acquired values plotted against weight.

After calibration, a testing instance was made to measure the value offsets for thrust and torque. This resulted in a thrust offset of 0.057 N and a torque offset of 0.004 Nm. Table III shows the percentage error for each data point in Fig. 12.

TABLE III
PERCENTAGE ERROR FOR EACH DATA POINT FROM THE MANUAL CALIBRATION OF THE SENSORS

Percent Error Torque	Percent Error Thrust
0.5%	0%
0.5%	0.00075%
0.5%	0.0008333%
0.875%	0.00025%
1%	0.0005%

3.4 Wind Tunnel Testing

In order to make use of data it first needs to verified. Even though the acquired testing rig can be calibrated with tools which were included, a second verification will be implemented to ensure correct data sampling. The wind tunnel test were

then divided into a section concerning the propellers and another concerning the motors.

3.4.1 Propeller Wind Tunnel Testing

The propellers were measured in the wind tunnel in order to get data to compare to the measurements in the UIUC database [18]. The propellers were run at the velocities expected in an actual mission. For each of the propellers, two test sessions were performed for 15 m/s and 22 m/s. No measurements where made at 35 m/s, the reason for this is explained in depth in 6.4.2. For each airspeed the angular velocity was varied roughly five times in order to measure propeller performance at a variety of advance ratios. Ideally, advance ratios ranging between 0.45 and 0.9 would be tested. At these points, propeller thrust, torque, and mechanical efficiency was recorded from the testing rig. Additional data such as temperature, density, and pressure was also recorded from the wind tunnel setup. This process was repeated for all the propellers, wind speeds, and angular velocities. The testing scheme is represented in the table IV.

TABLE IV
TESTING SCHEME FOR MEASURING DATA IN THE WIND TUNNEL

Constant	Vary	Measure	No. of measurements
Wind speed	Prop. angular velocity	Thrust	5 per prop. and wind speed
		Torque	
		Mechanical efficiency	
		Air density	
		Air temperature	
		Actual windspeed	

The sampling from the wind tunnel is continuously logged in the software for each measurement, and outputted as a table. In the post-processing phase, a MATLAB script was written where the data from the log from the software is looped through and divided up into the separate categories that are needed for the calculations. The program then calculates the mean of the torque, thrust, angular velocity, and motor efficiency values for each measurement which are then used for further calculations.

From the post processed data, coefficients and parameters such as C_T, C_Q, C_P, P and $\eta_{propeller}$ can be found by applying equations described in sections 2.1.2 and 2.1.3 to the test data. The resulting data is used to find new approximations of propeller parameters such as power consumption, propeller efficiency e.t.c at loiter which are useful for matching motors and estimating the propeller performance.

The tests were then processed and analysed from an error perspective. In order to find the margin of error a Matlab script was utilized. This script finds the uncertainty of measurements using Taylor and Monte Carlo simulations. The measured data is then inputted in the script as well as the assumed error for each variable.

The script outputs the error for the coefficient equation in question as well as the variable that contributes the most to this uncertainty.

3.4.2 Motor Wind Tunnel Testing

To verify data from motor screening the motors are tested for efficiency at different load points and angular velocity. This can be achieved by varying a torque load and angular velocity successively. This will be achieved by loading the motors with a propeller in a wind tunnel. The data for each loading point (torque and rotational velocity) will be extrapolated and averaged from approximately ≈100 data points collected at 20Hz frequency.

The propeller to be chosen for the tests will in this case be the propeller that was deemed most versatile throughout different angular velocities and wind speeds. Efficiencies of the motors throughout different angular velocities and wind speeds can then be found and displayed out in a heat map across torque and rpm axes as in Fig. 20. This will be achieved by performing a sweep of both wind velocities and angular velocities while measuring torque and efficiency at each point. The results could then be analyzed and matched to a propeller which would best fit the goals of the project.

4
Results

This chapter presents all the results from the propeller- and motor screening and selection processes, as well as the results from the rig design process and wind tunnel testing. They are presented in the form of tables and figures, where a major part of the propeller data tables can be found in appendix A, and wind tunnel test measurements in appendix C.

4.1 Initial Propeller Screening

In this section the results from the two initial propeller screenings in MATLAB are presented, as well as results from the take off capability verification. Figures and tables are used to both numerically and visually compare propellers and their performance in different scenarios, e.g different drone weights or velocities.

4.1.1 Pro-Propeller Selection

In table V the propellers that passed the first screening are listed.

TABLE V
PROPELLERS ACCEPTED IN PRO-PROPELLER SELECTION

Brand	**Model**	**D [Inches]**	**Pitch [Inches]**
Aeronaut	Carbon Electric	10	8
Aeronaut	Carbon Electric	11	10
Aeronaut	Carbon Electric	11	7
Aeronaut	Carbon Electric	11	8
APC	Thin Electric	11	8.5
Aeronaut	Carbon Electric	12	8
APC	Sport	10	7
Aeronaut	Carbon Electric	13	6.5
APC	Thin Electric	10	4.7
APC	Carbon Fiber	7.8	6
Aeronaut	Carbon Electric	10	12
APC	Thin Electric	9	6

Examples of the propeller graphs generated by the pro-propeller selection program

are shown below. Fig. 4.13a is an example of a graph from an Aeronaut 8.5x6 inches run at 15 000 rpm which is very close to its maximum of 16 000 rpm. The three rings represent the propeller performance at take off, loiter, and sprint respectively. Takeoff is the marker with lowest advance ratio, and sprint has the highest advance ratio. The program estimated that the propeller would deliver enough thrust, however the marker for sprint is badly placed in the figure, since it is detached from the UIUC measurements [18]. Therefore the propeller was rejected.

An efficiency curve for an accepted propeller is presented below in Fig. 4.13b. The graph shows $\eta_{propeller}$ for an Aeronaut Carbon Electric 11x10 inches run at 9000 rpm, where rings represent the propeller performance at takeoff, loiter, and sprint represented in the figure from left to right respectively. Here the flight mode markers are placed on the UIUC measurements [18], and the program also estimated that the propeller would deliver enough thrust in all flight modes.

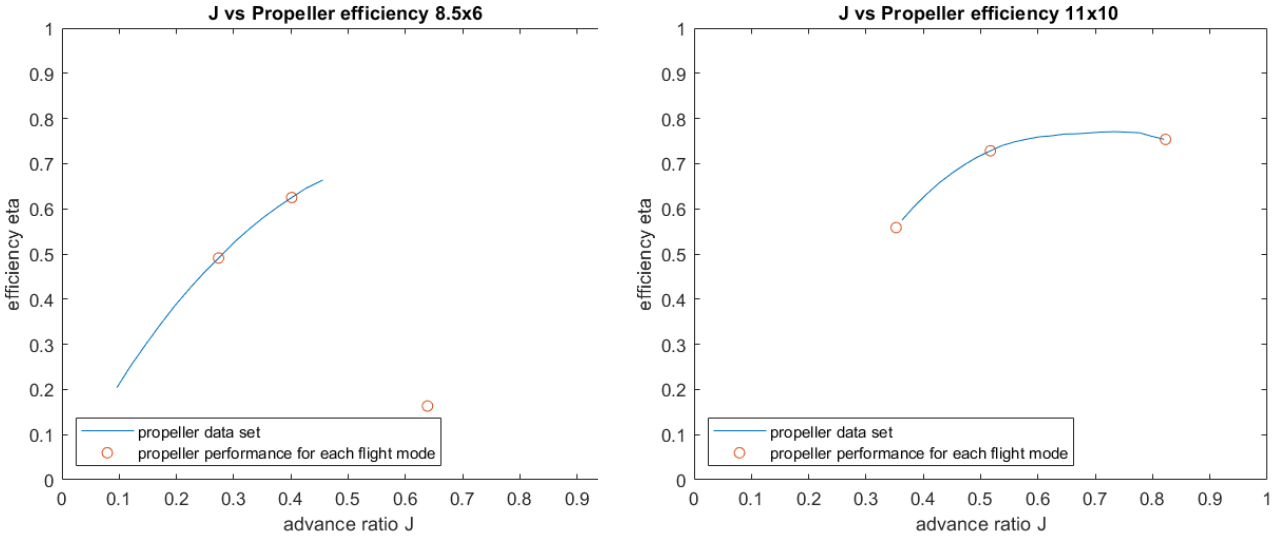

(a) Efficiency curve for Aeronaut Carbon Electric 8.5x6.

(b) Efficiency curve for Aeronaut Carbon Electric 11x10.

Fig. 13. Efficiency plotted against advance ratio for a rejected and an accepted propeller.

4.1.2 Propeller Downselection

Fig. 4.14a below shows the energy consumption for one entire mission, as specified in section 1.3.1, for all propellers that passed the propeller pro-selection and down-selection, plotted against the drone weight.

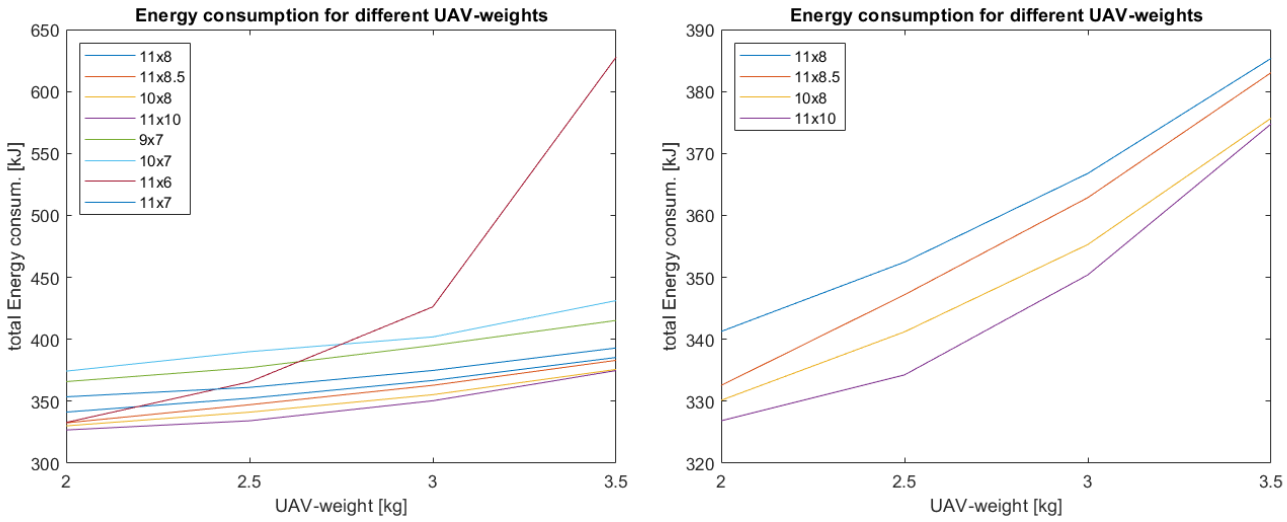

(a) Propeller energy consumption plotted against drone weight for all propellers.

(b) Top 4 propellers with lowest energy consumption for all drone weights.

Fig. 14. Energy consumption for varied drone weights.

As can be seen from Fig. 4.14a, the heavier the drone is, the more energy it consumes. The propellers that perform the best in this screening are the propellers with lowest energy consumption for all weights.
The top 4 best performing propellers in order are:

1. Aeronaut Carbon Electric 11x10
2. Aeronaut Carbon Electric 10x8
3. APC Thin Electric 11x8.5
4. Aeronaut Carbon Electric 11x8

Fig. 4.14b visualizes only the top four best performing propeller with lowest energy consumptions.

Table VI below shows data of the top four ranking propellers at UAV weight of 2.5 kg, produced by the program in propeller down-selection.

TABLE VI

TOP FOUR BEST PERFORMING PROPELLERS

Rank	**1**			**2**			**3**			**4**		
Propeller	**Aeronaut Carbon Electric 11x10**			**Aeronaut Carbon Electric 10x8**			**APC Thin Electric 11x8.5**			**Aeronaut Carbon Electric 11x8**		
UAV Weight [kg]	**2.5**			**2.5**			**2.5**			**2.5**		
Airspeed [m/s]	15	22	35	15	22	35	15	22	35	15	22	35
UAV AoA [deg]	9.31	3.32	0.48	9.31	3.32	0.48	9.31	3.32	0.48	9.31	3.32	0.48
UAV D [N]	1.62	1.53	2.97	1.62	1.53	2.97	1.62	1.53	2.97	1.62	1.53	2.97
Minimum Required T [N]	1.59	1.53	2.97	1.59	1.53	2.97	1.59	1.53	2.97	1.59	1.53	2.97
T [N]	1.91	1.55	2.97	1.61	1.56	3.02	1.60	1.57	3.02	1.59	1.55	3.00
C_T	0.06	0.03	0.02	0.05	0.03	0.02	0.04	0.02	0.02	0.04	0.02	0.02
C_P	0.06	0.04	0.04	0.05	0.04	0.03	0.04	0.03	0.02	0.03	0.03	0.02
P [W]	37.8	52.4	172.8	32.4	52.8	177.9	33.8	54.4	179.8	32.0	54.2	184.6
$\eta_{propeller}$	0.76	0.66	0.64	0.75	0.64	0.59	0.71	0.63	0.59	0.75	0.63	0.57
$\eta_{propulsive}$	0.95	0.98	0.98	0.95	0.98	0.98	0.96	0.98	0.98	0.956	0.98	0.98
η_{turbo}	0.83	0.78	0.77	0.79	0.66	0.61	0.72	0.51	0.35	0.74	0.40	0.15
n [rpm]	4000	4992	7770	4848	6236	9627	4595	6038	9357	4613	6056	9411
J	0.81	0.95	0.97	0.73	0.83	0.86	0.70	0.78	0.80	0.70	0.78	0.80
Time spent in mode [min]	0.5	40	20	0.5	40	20	0.5	40	20	0.5	40	20
Total Energy Consum. [kJ]		334.3			341.2			347.2			352.5	

From this table it can be seen that the energy consumption for one mission as specified in section 1.3.1 is around 345 kJ for a UAV weight of 2.5 kg. The maximum power consumption is around 177 W and occurs at sprint, and the optimal angular velocity varies between the propellers, but is at most around 9000 rpm. It can also be seen that the propeller- and turbo-efficiencies are quite low at loiter and sprint. It can also be seen that the propeller- and turbo-efficiencies increases with the rank of the propellers. In other words, propellers that have a high rank also have a relatively higher turbo-efficiency compared to the other propellers. The turbo- and propeller efficiencies are both lower for higher advance ratios. The propulsive efficiency however is quite high and increases with higher advance ratios. Additional data for the top four best performing propellers for different weights and stable flight are found in the appendix A.

The propeller efficiencies at takeoff, loiter, and sprint for an 11x10 propeller can be found in Fig. 4.15a. The propeller efficiencies are plotted left to right for takeoff, loiter and sprint respectively. The performances at these flight modes at a drone weight of 2.5 kg are plotted on top of the propeller data set from the UIUC database. [18].

The propeller efficiency measured in the UIUC [18] database for the Aeronaut Car-

bon Electric 10x8 propeller is plotted in Fig. 4.15b below. Takeoff, loiter, and sprint propeller efficiencies are plotted left to right respectively at drone weight of 2.5 kg on top of the database measurements.

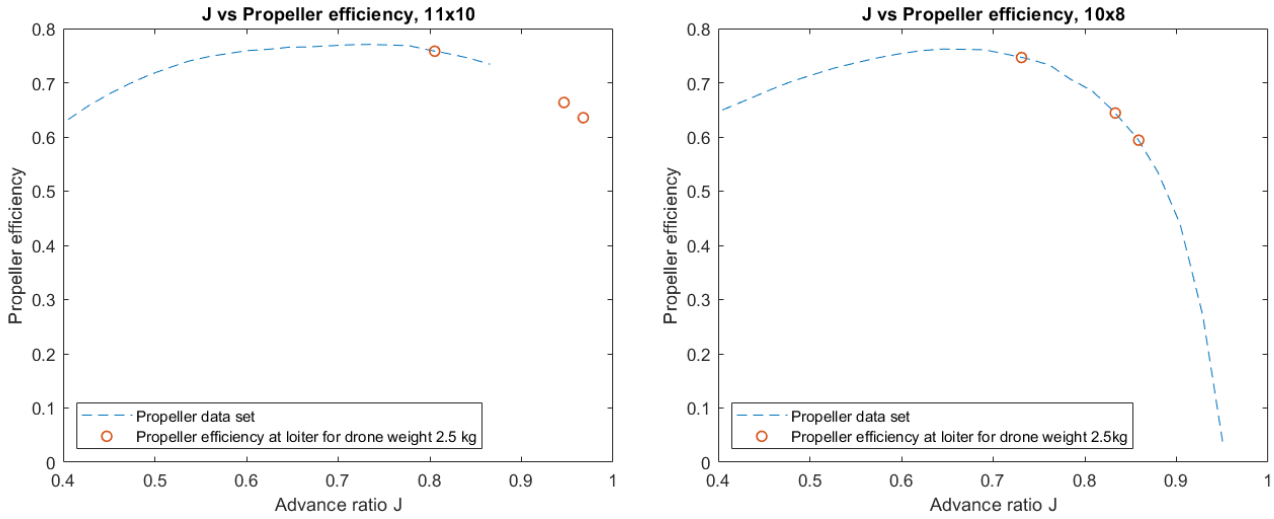

(a) Propeller efficiency curve for Aeronaut Carbon Electric 11x10 inches, at drone weight of 2.5 kg.

(b) Propeller efficiency curve for Aeronaut Carbon Electric 10x8 inches, at drone weight of 2.5 kg.

Fig. 15. Efficiency plotted against advance ratios for two different propellers.

In Fig. 4.16a the propeller efficiencies measured in the UIUC database [18] for all the top four propellers are plotted against the advance ratio J. In Fig. 4.16b the turbo-efficiencies of the top four propellers are plotted against the advance ratio. The operational propeller and turbo-efficiency for loiter at a drone weight of 2.5 kg is also marked in the figure for every propeller.

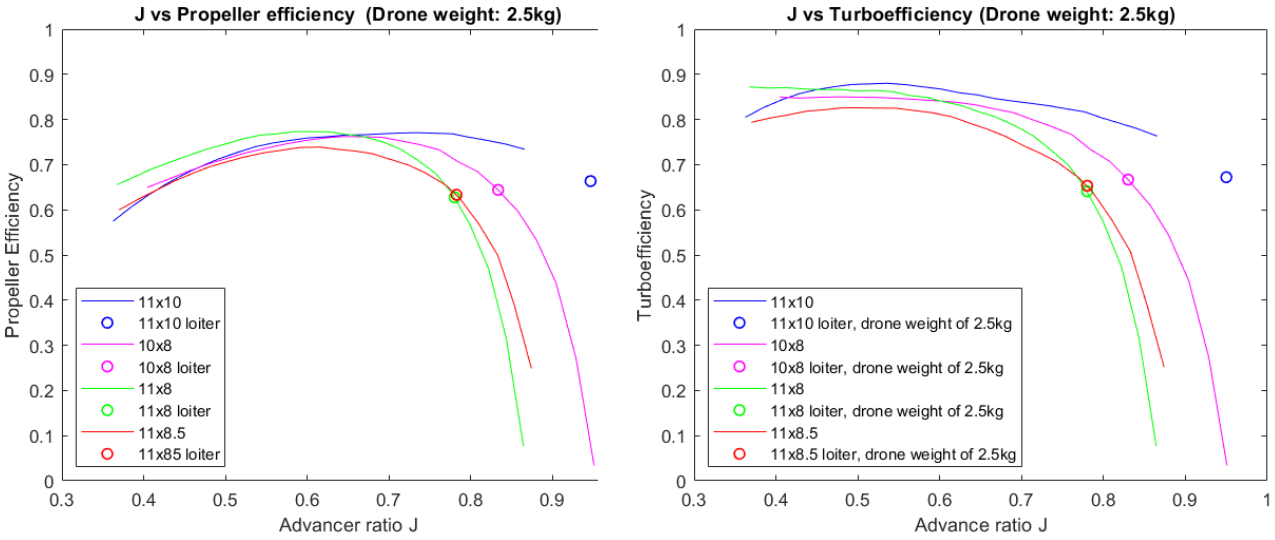

(a) Propeller efficiencies for the selected top four propellers plotted against the advance ratio.

(b) Turbo-efficiencies for the selected top four propellers plotted against the advance ratio.

Fig. 16. Two different measures of efficiency plotted against advance ratio.

From Fig. 4.16a it can be seen that the propeller efficiency for the best ranked propeller, the Aeronaut Carbon Electric 11x10, has its peak at higher advance ratios compared to the other propellers. The worst performing of the top four propellers, the Aeronaut Carbon Electric 11x8, has its efficiency peak at lower advance ratios.

The turbo-efficiency visualized in Fig. 4.16b behaves similarly to the propeller efficiency. The best performing propeller in terms of energy consumption has its turbo-efficiency peak shifted towards higher advance ratios compared to the other propellers. From Fig. 4.16a and Fig. 4.16b it is observed that the turbo- and propeller efficiencies are low, and located at higher advance ratios than the efficiency peaks.

In Fig. 17 the efficiency for the Aeronaut Carbon Electric 10x8 at loiter has been plotted for two different drone weights, 2 and 2.5 kg, on top of the efficiency measurements from the UIUC database [18].

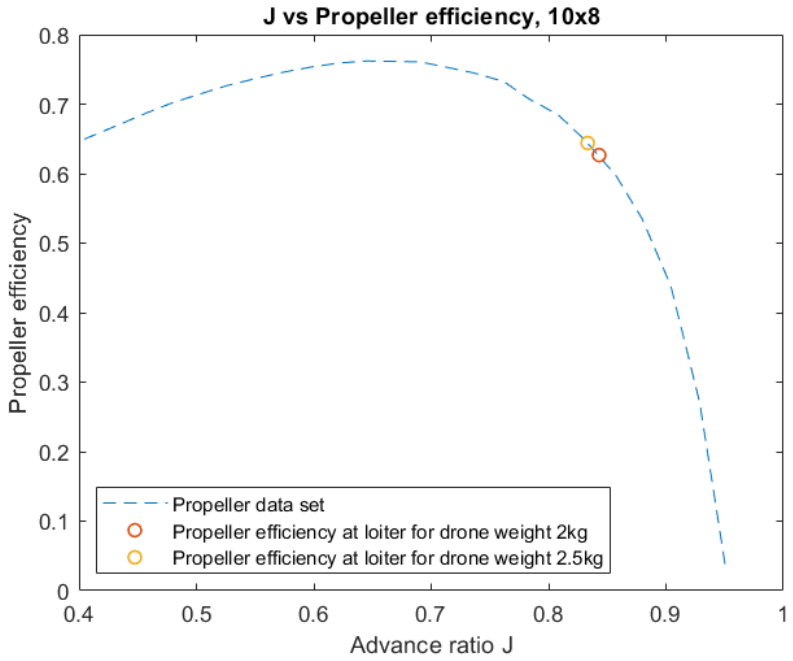

Fig. 17. Efficiency at loiter for Aeronaut Carbon Electric 10x8 inch at loiter for UAV weight of 2 and 2.5 kg.

Here it can be observed that a drone weighing 2.5 kg operates at a lower advance ratio than a drone weighing 2 kg. Also it can be observed that a heavier drone operates at a higher propeller efficiency than a lighter drone.

4.1.3 Takeoff Capability

The data produced by the takeoff capability program in 3.1.5 is listed in table VII.

TABLE VII
PROPELLER TAKEOFF PERFORMANCE AT 2.5 KG

Propeller rank	**1**	**2**	**3**	**4**
Propeller	**ancf 11x10**	**ancf 10x8**	**apce 11x8.5**	**ancf 11x8**
T [N]	18.77	11.12	14.52	14.70
Forward Net Force [N]	16.96	9.43	12.78	12.95
Forward Acc. [m/s^2]	6.78	3.77	5.11	5.18
Lift [N]	25.72	25.72	25.72	25.72
Upward Net Force [N]	1.17	1.17	1.17	1.17
Upward Acc. [m/s^2]	0.47	0.47	0.47	0.47
P [W]	489.64	256.67	363.83	336.16
n [rpm]	8882	8759	8706	8764
Acc. Time to Sprint [s]	2.95	5.31	3.91	3.86

The results table VII are notably different than the takeoff columns in table VI, since in this scenario the drone is in maximum acceleration. Here it can be seen that the angular velocity is closer to 8800 rpm than 4000 rpm, and the power required is around 350 W.

4.1.4 Propeller Initial Selection Summary

The data computed can be summarized as:

- The maximum propeller power expenditure at stable flight occurs at sprint and is estimated to be around 175 W. For takeoff, where the drone accelerates, the power consumption may be even higher.
- The propeller are run at roughly 5000 - 6000 rpm at loiter and 9000 rpm at sprint. For takeoff this number can vary dependent on how the max power expenditure of the motor.
- The total energy consumption for 1 hour of flight is estimated to roughly 340 kJ.

Now that an initial selection of four propellers is made they are purchased, and tested in the wind tunnel in order to more accurately specify the best propulsive configuration for the drone. The data and information from this section is also useful in order to find suitable motors that work well together with the propellers. The motors and propellers are tested in a wind tunnel in the exact conditions expected during a rescue mission, to measure their performance and compare it to the data in the UIUC database [18].

4.2 Motor Screening

As described in 3.2, the motor screening is divided into two processes. The first eliminated all the motors that could not meet the requirement of the drone. The second ranked them from what was deemed as the best performing to the worst performing.

4.2.1 Elimination Screening

The requirements that had to be met from a propeller aspect can be seen in table VIII.

TABLE VIII
REFERENCE PROPELLER CRITERIA

Reference Propeller Carbon Electric 11x10	
Takeoff n [rpm]	6683
Loiter n [rpm]	4992
Sprint n [rpm]	7770
Takeoff power [W]	212.45
Loiter power [W]	52.39
Sprint power [W]	172.82

If a motor could perform at this level according to its technical specifications, it was accepted. The load under takeoff was exempt, in other words if the motor performed well in all the other modes but under-performed in takeoff, it could still be taken into consideration. This resulted in an elimination of 12 motors out of a total of 43.

The second criteria motors were eliminated based on was the torque matching criteria, as mentioned in 3.2.2. This criteria further eliminated 11 motors, making the total eliminated motors 23 out of the total 43. The top 20 performing motors were then ranked as mentioned previously.

4.2.2 Ranking of the Top Performing Motors

The motors were ranked with the criteria in section 4.2. The observed final ranking are presented in table IX.

TABLE IX
THE FINAL RANKING OF THE MOTORS, WHERE A HIGH SCORE SIGNIFIES A GOOD PERFORMANCE OF THE MOTOR

Motor Name	Score out of 140
GT2826/06	98
GT4020/09	94
GT2826/05	94
GT3520/05	92
GT3526/05	91
GT2820/07	89
GT3526/04	87
GT2820/06	82
GT2812/08	79
GT2820/05	77
GT2815/07	76
GT2812/09	75
GT2820/04	73
GT2815/06	72
GT2826/04	71
GT2812/10	69
GT2812/06	69
GT2218/09	66
GT3520/04	60
GT2815/05	48

For reasons presented in chapter 6, the chosen five top candidates from this list are:

1. GT2826/05
2. GT3526/05
3. GT2820/07
4. GT3526/04
5. GT2820/06

4.3 Wind Tunnel Testing

This section reveals the results from the wind tunnel testing. These results were then combined and used to match the propeller and motors, which are presented in this section as well.

4.3.1 Propeller Wind Tunnel Measurements

In this section the results from the measurements of the propeller 10x8 Aeronaut Carbon Electric in the wind tunnel are presented. Tables X to XIII present the measured and derived values for wind speeds 15 m/s and 22 m/s.

In table X the measurements made in the wind tunnel for the Aeronaut Carbon electric at 15 m/s 10x8 are listed.

TABLE X
10x8 15 m/s Wind tunnel measurements

Measured V [m/s]	**Measured n [rpm]**	Q [N/m]	T [N]	η_m
15.09	4002	0.021	0.041	0.449
15.11	4635	0.047	0.850	0.539
15.15	4856	0.056	1.136	0.566
15.17	5010	0.063	1.359	0.588
15.19	5640	0.092	2.282	0.648
15.25	7162	0.159	4.974	0.696
15.33	8477	0.238	8.238	0.736

In table XI the propeller coefficients that can be derived from the measurements in table X are listed.

TABLE XI
10x8 15 m/s Derived propeller data

J	C_T	C_Q	C_P	P [W]	$\eta_{Propeller}$
0.905	0.002	0.004	0.025	8.79	0.070
0.782	0.030	0.007	0.042	22.84	0.562
0.749	0.037	0.007	0.046	28.60	0.602
0.727	0.041	0.008	0.048	32.99	0.625
0.646	0.055	0.009	0.055	54.13	0.640
0.511	0.074	0.010	0.060	119.51	0.635
0.434	0.088	0.010	0.064	211.05	0.598

In table XII the measurements made in the wind tunnel for the Aeronaut Carbon electric 10x8 at 22 m/s .

TABLE XII
10x8 22 m/s Wind tunnel measurements

Measured V [m/s]	**Measured n [rpm]**	Q [N/m]	T [N]	η_m
22.3	5766	0.043	0.231	0.523
22.3	6489	0.086	1.477	0.625
22.3	7414	0.148	3.271	0.719
22.3	8646	0.236	6.191	0.781
22.3	8985	0.264	7.144	0.802

In table XIII the propeller coefficients that can be derived from the measurements in table XII are listed.

TABLE XIII
10x8 22 m/s Derived propeller data

J	C_T	C_Q	C_P	P [W]	$\eta_{Propeller}$
0.928	0.005	0.004	0.025	25.87	0.199
0.825	0.027	0.006	0.039	58.13	0.567
0.722	0.046	0.008	0.052	114.81	0.635
0.619	0.064	0.010	0.061	214.04	0.645
0.596	0.068	0.010	0.063	248.40	0.641

The parameters J, C_T, C_P, and $\eta_{propeller}$ from table XI and table XIII are plotted against the corresponding data from the UIUC database [18]. This is done in order to compare the wind tunnel measurements to the data points in the database. The plot for the thrust coefficient can be seen in Fig. 4.18a, the power coefficient in Fig. 4.18b, and the propeller efficiency in Fig. 19. Also included in the figures are the estimated errors due to noise for the 15 m/s samples, these are visualized as error bars.

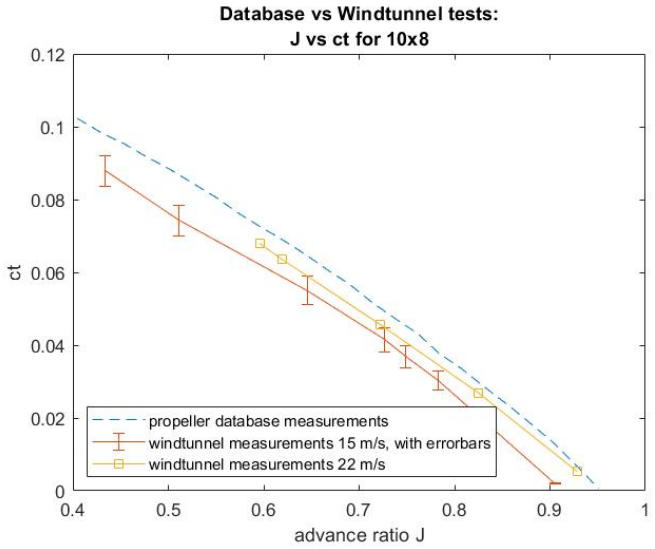

(a) Thrust coefficient derived from wind tunnel measurements for 10x8 propeller.

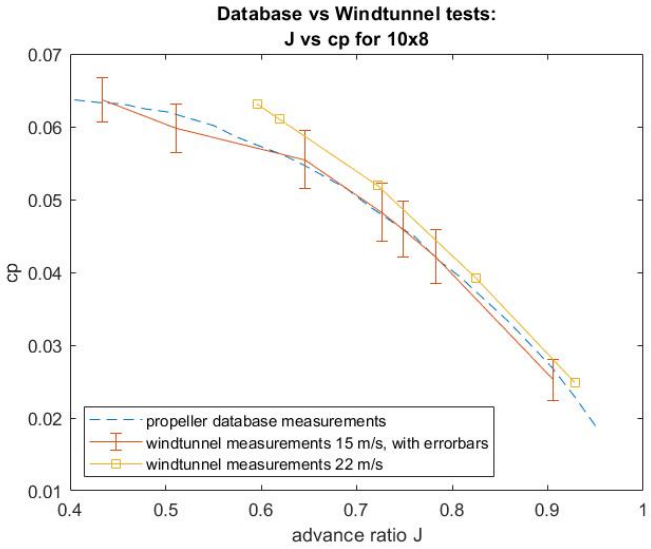

(b) Power coefficient derived from wind tunnel measurements for 10x8 propeller.

Fig. 18. Derived propeller coefficients from wind tunnel measurements.

From Fig. 4.18a it is observed that the thrust coefficient measured in the wind tunnel is slightly lower than the UIUC measurements [18], however it follows the same trend. The power coefficient for 15 m/s closely resembles the UIUC database measurements, however the measurements done at 22 m/s indicate a higher power coefficient than the UIUC database.

Fig. 19shows the propeller efficiency for the wind tunnel measurements is significantly lower than the UIUC propeller efficiency.

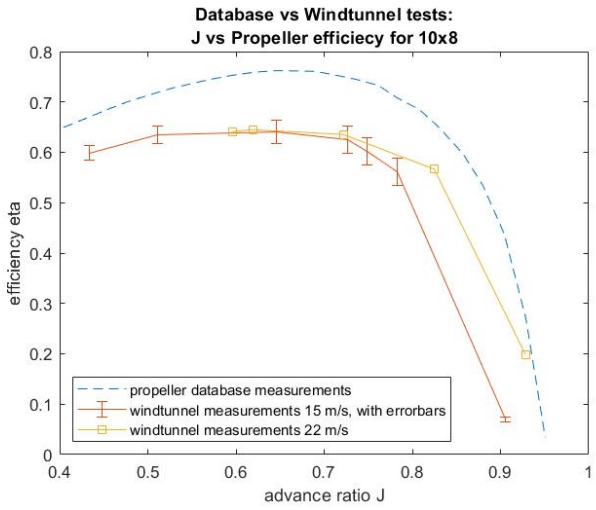

Fig. 19. Propeller efficiency derived from wind tunnel measurements for 10x8 propeller.

The observed error ultimately depends on the large noise received in the angular velocities observed. The angular velocity noise detected is to be around ± 200 rpm, this causes it to be the primary factor in the calculated uncertainty. The noise uncertainty was chosen due to its large impact on the data whereas the bias error had a smaller contribution. As seen in Fig. 4.18a the uncertainty of C_T was found to be around 7% whereas in figure 4.18b C_P was found to be around 7% as well. The propeller efficiency in figure 19 was found to be around 6%.

The results for the other propeller models, except Aeronaut Carbon Electric 11x10 can be seen in appendix C. The reason the results from the wind tunnel tests of the 11x10 are not included in this report is due to the results from the measurements being inconclusive. This is further explained in section 6.4.2.

Using the wind tunnel measurements, new estimates of the torque, propeller efficiency and power consumption are made, for the thrust requirement computed in 3.1.4 step 3. In table XIV these parameters are listed for the thrust requirement at loiter for a drone weighing 2.5 kg.

TABLE XIV
ESTIMATIONS OF PROPELLER PARAMETERS BASED ON WIND TUNNEL MEASUREMENTS, FOR A DRONE WEIGHING 2.5 KG OPERATING AT 22 M/S

Rank, least power consum.	**1**	**2**	**3**
Propeller (size x pitch) [inches]	**10x8**	**11x8**	**11x8.5**
Required T [N]	1.53	1.53	1.53
J	0.821	0.789	0.791
n [rpm]	6430	6073	5975
$\eta_{propeller}$	0.572	0.540	0.508
Q	0.088	0.099	0.106
Estimated P [W]	52.80	54.20	54.40
Measured P [W]	59.71	62.99	66.28
P increase [%]	13.08	16.22	21.84
Measured η_m [%]	62	67	71
Measured P_m [W]	93.20	95.30	99.20
Ideal P_m [W]	57.90	63.85	70.43

In this table it can be seen that the power consumption is the lowest for the 10x8 propeller, 59.71 W at loiter, which is an increase of about 13% compared to the power consumption approximated in table VI. The propeller efficiency estimated for loiter at 2.5 kg is around 53% for the 10x8 and the angular velocity is around 6430 rpm. The table lists the motor power and efficiency values recorded from the software, and what the ideal power consumption would be if the motors had a 100% efficiency.

4.3.2 Motor Efficiency Measurements In Wind Tunnel

Testing of the motor efficiency was done accordingly to the method description. Out of the planned motor only three were tested due to time constraints. The motors tested were GT2820/06, GT2820/07, and GT2826/05. Heat maps were created for each motor which can be seen in Fig. 20.

It is noted that GT2826/05 is the least efficient of the three motors tested, with a peak efficiency of about 75% at an angular velocity of 6538 rpm and a torque of about 0.1951 Nm. The the most efficient motor GT2820/07 peaks at about 86% at an angular velocity of 6311 rpm and a torque of about 0.1697 Nm. However, it is important to note that the angular velocity sensor is not entirely accurate as can be observed in the standard-deviation heat map of the angular velocity on the right of Fig. 20.

The standard deviation graphs show where the collected data points have a large standard deviation which in simple terms means that the angular velocity measurements are not precise. This is discussed further in 6.4.2.

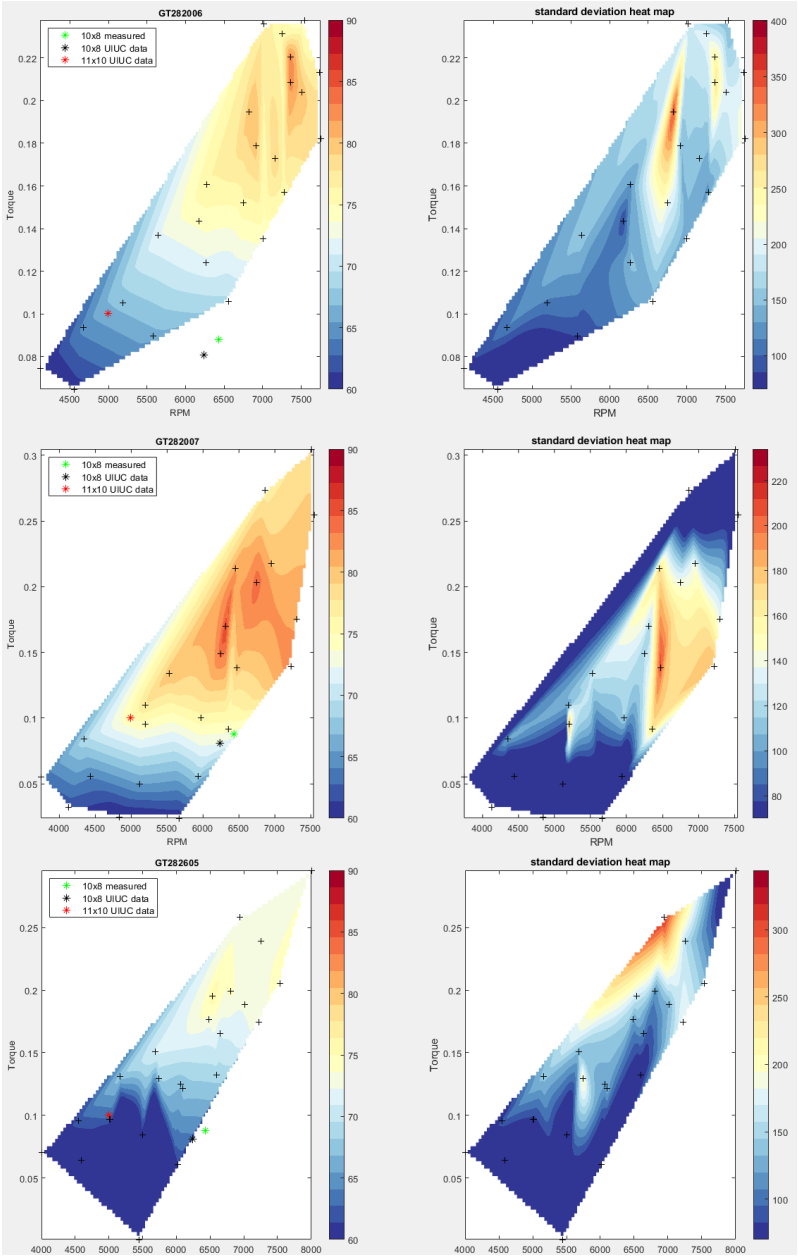

Fig. 20. Left: Heat maps of motors tested. Right: Standard deviation error plot of the respective motors. "+" marks the scattered torque and angular velocity data points collected.

4.3.3 Propeller-Motor Matching

The torque and angular velocity of the top two propellers, 10x8 and 11x10, selected in section 3.1.4 at loiter at 2.5 kg drone weight are plotted together with the motor heat map. Due to failed tests that are analysed in section 6.4.2, the data for the propeller Carbon Electric 11x10 was taken from parameters in table VI. The torque and angular velocity for loiter of the 10x8 based on the wind tunnel measurements is plotted, as well as the torque and angular velocity for loiter based on table VI. This is in order to compare the the motor matching between the UIUC based propeller parameters and the wind tunnel based estimates of torque and angular velocity at loiter.

In Fig. 21 the propellers work load is marked in the heat maps for loiter at 2.5 kg drone weight, and almost all of them fall outside of the motors optimal efficiency range. It can be seen that the best motor is GT2820/07 as the efficiency reaches upwards 75% for almost all propellers, though at different angular velocities.

In Fig. 22 the propellers work load is marked on the motor heat maps for sprint at 2.5 kg drone weight. Almost all of the propellers fall outside of the motors optimal efficiency range as well. The best motor-propeller match is GT2820/06 and 11x10 with an efficiency of around 80%. It should be noted that the data points for the heat-map does not include the span of angular velocities that the propellers operate at for sprint, or the efficiency at these operating points.

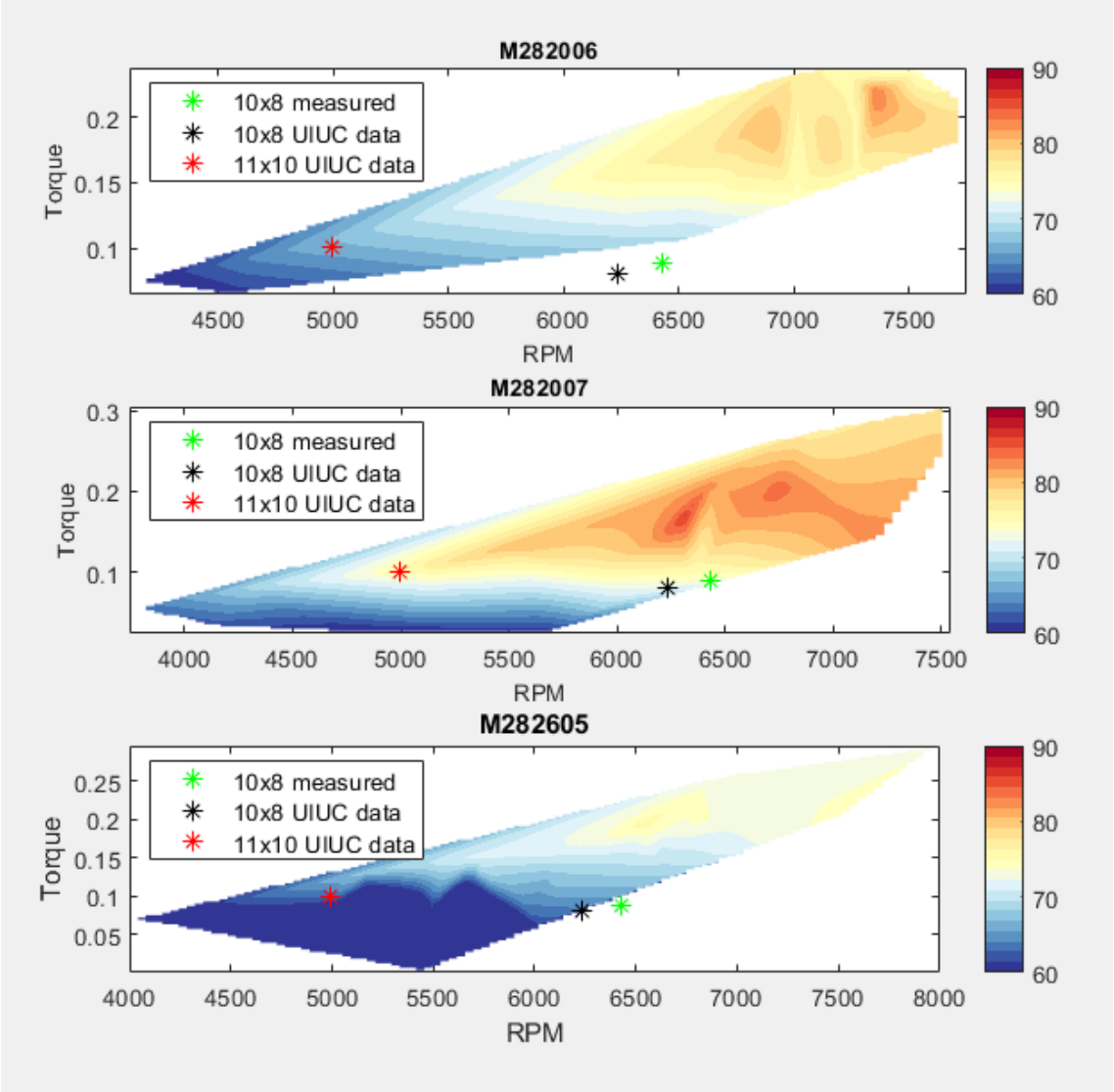

Fig. 21. Propeller data for loiter plotted with asterisks on the heat map to distinguish motor-propeller efficiency match.

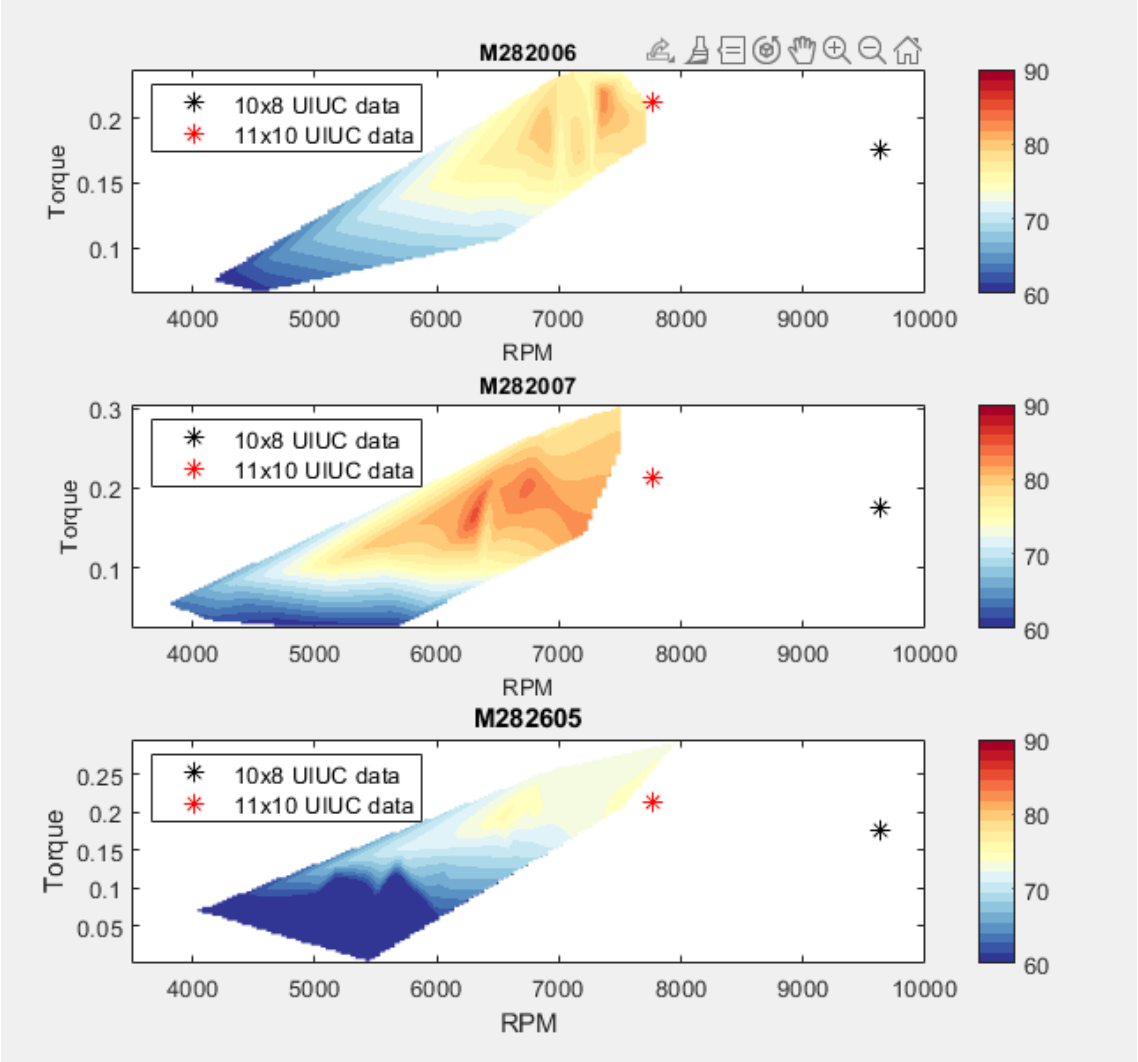

Fig. 22. Propeller data for loiter plotted with asterisks on the heat map to distinguish motor-propeller efficiency match.

5

Discussion

In this chapter the results from the propeller and motor screenings as well as results from the wind tunnel tests are examined, interpreted, and discussed. Topics such as propeller performance and motor-propeller compatibility are also examined. This chapter also concludes with a discussion whether or not the purpose of the project has been fulfilled.

5.1 UAV Weight

Since this project is still in its prototype phase, it is unknown exactly how much the final UAV will weigh. The initial estimation was that the drone would weigh 2.5 kg, but the new estimations are closer to 3 kg. The weight of the drone has a great influence on the energy consumption of the propeller, which can be seen in (18). Therefore the estimation of propeller performance for a range of different weights is useful for predicting how the UAV performs, with regards to the uncertainty in the final drone weight.

In table XIX a useful observation can be made. At 2.5 kg the drone angle of attack needed to maintain stable flight at takeoff is 9.3°, which is close to the stalling safety limit of 10°. At 3 kg the takeoff angle of attack is 12.6° and exceeds the limit. This occurs independently of the propeller and is purely an aerodynamic issue. This means that in order for the drone to be able to maintain stable flight at takeoff for 3 kg, the reference area needs to be increased, which is outside the scope of this project. This means that the this project will focus on the propellers that perform the best for a drone weighing maximum 2.5 kg.

5.2 Propeller Selection

In this section the conclusions from the propeller selection process are interpreted, assessed, and discussed. Topics such as takeoff capability as well as propeller-, turbo-, and propulsive efficiency are discussed in this section, based on the results from the propeller screening.

5.2.1 Propeller Screening

The results from the propeller screening presented in table VI as well as Fig. 4.14b indicate that the best performing propeller for this particular application is the Aeronaut Carbon Electric 11x10 inches. Out of all the assessed propellers, the 11x10 is considered to have the lowest energy consumption per mission, which was the criterion to be minimized. Other results such as Fig. 4.16a and Fig. 4.16b reinforces this resolution, by indicating that the 11x10 propeller has the highest turbo- and propeller efficiency for loiter at a drone weight of 2.5 kg. This coincides with the theory, that a low energy consumption also occurs at high propeller-, turbo-, and propulsive efficiency. Therefore the results in the propeller screening process indicate that the 11x10 propeller is considered a good match for the UAV evaluated in this project.

For the Aeronaut Carbon Electric 11x10, there is a lot of uncertainty regarding the values computed in section 3.1.4. As can be seen in Fig. 4.15a, the advance ratios at which the propeller operates at loiter and sprint are well outside the advance ratios measured in the propeller database. Normally a propeller with operational advance ratios that far outside the measured range would be rejected, but for this propeller an exception was made for a few reasons. First and foremost the values for $\eta_{propeller}$, C_T, and C_P seem to follow the trend in the plot by extrapolation as can be seen in Fig. 4.15a. Secondly, the values for C_T and C_P were above zero and seemed reasonable. Lastly, the 11x10 performed very well compared to the other propellers in the selection process. Therefore it was selected for further testing, despite there being a risk of the coefficients and parameters produced in the selection process being inaccurate.

5.2.2 Takeoff Capability

One important insight can be found from the required power computed for takeoff in table VII. It is almost double the maximum sprint power in stable flight, and this can be problematic since it might be too high for an electric motor to deliver. This can be remedied by decreasing the angular velocity, which in turn reduces the power needed to an acceptable level for the electric motor. The penalty for doing this is reduced thrust and therefore increased acceleration time, but since it is already very short in this scenario, it poses a problem. The results indicate that for takeoff the electric motor is the limiting factor, and for this application it is better to reduce takeoff acceleration to a level that a motor optimized for loiter and sprint can handle.

The takeoff lasts for a very short period of time, so there is no need to optimize for energy consumption since the contribution to the overall consumption is negligible. It is more reasonable to optimize the propeller for loiter and sprint instead. The only criteria in takeoff is that the propellers can deliver enough thrust for the drone to fly and accelerate, which the results in table VII indicate.

Even if the drone is optimized for flight with low energy consumption, it is completely essential that it will manage takeoff, otherwise the UAV will not reach the

other flight modes and complete its mission. The upward acceleration time is difficult to estimate since it is unknown how high the drone needs to climb, it might even vary between every mission. However, the results in table VII indicate that the drone is able to climb, which is an important observation.

5.2.3 Propeller Performance

One of the aims of this project has been to find the propellers with the lowest power and energy consumption. In this project this has been done by selecting propellers and their angular velocities such that they produce enough thrust but with lowest possible power consumption. Theoretically, this should also mean that all the different measures of efficiency should be high, however the result indicate low turbo- and propeller efficiencies for the selected propellers. In this section the propeller-, propulsive-, and turbo-efficiencies of the propellers assessed in the project are discussed.

Propulsive Efficiency

As can be seen from the results in table VI, the propulsive efficiency for all propellers is high, at around 98%. The high propulsive efficiencies presented in table VI are likely due to the fact that the propeller diameters are large compared to the thrust they produce.

Propeller Efficiency

Ideally the propeller operational points would be situated near the efficiency peak, in order to maximize the thrust to power ratio which in turn would minimize the power expenditure. The propellers assessed for this application have been shifted to the right, resulting in higher operational advance ratios than optimal which results in relatively low propeller efficiencies. This can be seen from all the figures representing the relationship between $\eta_{propeller}$ and J, for example see Fig. 4.16a.

The main reason that the propeller efficiency is low is that there is a mismatch between the operational advance ratio and the propeller efficiency peak. In other words, the efficiency peak of the propeller occurs at a different advance ratio than where the propeller operates. In this particular case the efficiency peak occurs at a lower advance ratio than where the drone operates. This means that the parameters affecting the advance ratio also have an effect on the efficiency. From (3) it is apparent that the advance ratio is dependent on parameters such as velocity, angular velocity and propeller diameter. This means the low propeller efficiency can in part be credited to the propeller not being optimal for the parameters defined by the drone mission specification in section 1.3.1.

Another parameter that implicitly has an effect on the propeller efficiency is the drone weight. During a mission, the drone must maintain stable flight, meaning

that thrust has to exactly match the retarding forces such as drag. The drag is dependent on the lift, which in turn has to match the self weight of the drone. This means that a heavier drone requires more thrust which occurs at a lower advance ratio. In other words a heavier drone operates at lower and more efficient advance ratios. This is visible in Fig. 17, where the efficiency for a drone weight of 2.5 kg is higher than the efficiency for 2 kg. It can be concluded that the propellers available in the UIUC database [18] are a better fit for applications where more thrust is required, than what is required for this particular UAV.

Turbo-Efficiency

Similarly to the propeller efficiency, the turbo-efficiency is generally low for the propellers in the top four selection, as can be seen in fig. 4.16b. This means that the change of the kinetic energy in the air behind the propeller is not efficiently used to move the UAV forward, and the propeller consumes more shaft power than necessary. Improving the turbo efficiency would therefore reduce the power consumption and would overall have a positive effect on the performance of the UAV. The results in 4.16b suggest that the turbo-efficiency peak is situated at lower advance ratios than where the drone operates, similar to the propeller efficiency. This means that the same parameters (such as weight, angular velocity and wind speed) that affect the advance ratio and propeller efficiency likely also have an effect on the turbo-efficiency.

5.3 Initial Motor Screening

In this section, topics concerning the motor screening and selection are discussed. The methods used and the results achieved are discussed and examined and expectations of the motor testing phase can be hypothesised.

5.3.1 Motor Rankings

The motors selected after the eliminations provide a range of different characteristics, as mentioned previously in 3.2, to be examined. This leads to a testing phase where more information can be deduced about how a specific motor will perform under load. It can be deduced from the preliminary screening as well as the motor equations in 2.2.1 that a motor with a higher motor constant and relatively low internal resistance will be a better suited motor for the UAV evaluated in this project. This can be a direct link to the number of coils due to its correlation to resistance. Motors with higher motor constants tend to perform worse in the areas of high current demand. The weight of the motor is also an important aspect as it is directly correlated to power consumption through several aforementioned factors in section 5.1.

5.4 Wind Tunnel Measurements

This section discusses the results observed and measured in the wind tunnel. This includes a discussion of the propeller- and motor measurements, as well as the combinations of the components.

5.4.1 Propeller Measurements

The results from the wind tunnel measurements in table XIV suggest the 10x8 is the best performing propeller in terms of power consumption out of the three propellers tested. It also has the highest measured propeller efficiency at 57% for loiter at a drone weight of 2.5 kg.

From table XIV it is visible that the power consumption estimated from the wind tunnel measurements is significantly larger that the power consumption estimated in table VI. The higher torque and power measurements lead to a C_p value which shows to be inconsistent with the data from UIUC propeller database. The higher power draw could be a result of multiple variables, including but not limited to, inefficient cabling, overheating of the ESC, or that the cables of the test rig's sensors were taken out of their sockets when putting together the test rig. The propeller efficiency of the propellers is also notably lower than the expected values from the propeller screening. An inconsistency in the value of the power draw leads to inconsistencies in other values, such as torque and efficiency which is presumably the case here. Regardless of the issues that occurred, the trends observed from the acquired data lie within what is expected.

5.4.2 Motor Measurements

The motor heat maps are not entirely conclusive as the angular velocity values turned out to be inconsistent at certain intervals. The data however shows a general trend, as shown in Fig. 20; all motors seem to have an optimal efficiency range for certain torques and angular velocities despite the inconsistency. In general all motors need to be loaded with a certain torque at a certain angular velocity to achieve their maximum efficiency. This is a normal occurrence in many propulsive systems and in some cases is mitigated by a continuously variable transmission to run a propulsive system continually and only in its peak efficiency. For the project it is of interest to match this high efficiency area with the required torque and angular velocity of a propeller to achieve the required thrusts while minimizing power consumption. It can also be mentioned that the final ranking differs from that of the screening process due to the uncertainties in motor screening as mentioned in section 6.2.2.

5.4.3 Measured Propeller-Motor Compatibility

In section 4.3.3 different motor-propeller combinations were optimal for different load cases. For loiter a clear motor candidate was GT2820/07 for any of our chosen

propellers. In sprint there was no way to objectively choose a motor and propeller as the load cases fell outside the heat maps data span. If forced to choose a motor and propeller by a competent and educated guess the choice for motors would fall between the GT2820/06 and GT2820/07. The carbon Electric 11x10 would be chosen as its work load based on VI is nearest the heat-map data span, however, there is limited to no data to indicate any motor efficiency drop-off at higher angular velocities. Another competent guess would suggest that the efficiency might drop off after 8000 rpm and thus omitting the 10x8 as a choice in sprint.

In section 3.1.4 and in table VI the propellers were chosen based on minimum total energy consumption. The table does not include the energy consumption for different load cases but they are easily derived from direct energy consumption (in watt) and time to fly. In simplest terms the energy consumption for sprint is twice as high than loiter which essentially means that the propulsive system ought to be optimised for sprint. Without the possibility to test the motors properly with an accurate torque-brake it was not possible to choose propellers-motor combination with good accuracy though our data gives us a good enough approximation.

6
Conclusion

This chapter includes conclusions about the motor and propeller selection process, as well as conclusions regarding the project as a whole. Here conclusions regarding the theory and methods used are presented, as well as conclusions regarding the results. Suggestions on what could have been done differently in this project are also covered, as well suggestions and recommendations for future projects.

6.1 Propeller Selection

In this section, conclusions regarding the propeller selection are made, based on the results and discussion. Topics such as suggested methods to improve propeller efficiencies, as well further research suggestions and error surveys are also introduced in this chapter.

6.1.1 Propeller Recommendations

Since the measurements made in the wind tunnel for the 11x10 were inconclusive, the uncertainty regarding this propeller is even greater compared to the other propellers measured. For that reason it is difficult to make a final verdict regarding which propeller would perform best on this UAV. It can be said however that the the 10x8 is a good option based on the wind tunnel measurements as well as the results in table VI, and this is consistent with it being the second best option after the 11x10 in the screening process. To summarize, the propellers available on the market which are best fitted for the UAV mission defined in 1.3.1, are the Aeronaut Carbon Electric 10x8 and 11x10. This recommendation is made based on the results in tables VI and XIV.

6.1.2 Propulsive Efficiency

Since the propulsive efficiency is very high, it is unlikely that increasing it even more would have any dramatic effects on the UAV overall performance. In contrast it might even have negative effects on the UAV's overall performance, especially when it comes to maneuverability. In order to maximize propulsive efficiency, large propellers operating at high wind speeds are favoured. But there is a limit to how much torque an aircraft can handle, and a larger propeller has a tendency to induce more torque which can negatively affect maneuverability.

6.1.3 Improving Turbo- and Propeller Efficiency

There is an interest in improving the propeller- and turbo efficiency, as the results suggest that it is low for the current selection of propellers. Improving the propeller- and turbo efficiency would mean that the UAV consumes less power for each mission. Since the propeller efficiencies are low as a result of a mismatch in the operational advance ratio and the efficiency peaks, this is where improvement measures should be applied.

There are two main ways to match the operational advance ratio with the efficiency peaks. Either the operational advance ratio is reduced, or the efficiency peaks should be translated to a higher advance ratio. Since the mission velocities are predefined, only the diameter, pitch and angular velocity of the propeller may be altered. The suggested strategies to do this are described below.

- **Decrease operational advance ratio:** One way to reduce the advance ratio is to increase the angular velocity of the propeller, see (3). In order to increase angular velocity and maintain stable flight propeller pitch also has to be decreased. A lower pitch will allow the propeller higher angular velocity without producing too much thrust. This is in order to keep the drone in equilibrium. However a lower pitch also means that the efficiency peak occurs at yet a lower advance ratio, see fig.6. In order to 'make up for' this, the propeller diameter might also have to be increased, however it must be noted that this might have a negative effect on the torque as discussed earlier in this chapter.

- **Increase advance ratio of efficiency peaks:** As visualized in Fig.6, the propeller efficiency can be translated to higher advance ratios by increasing the propeller pitch. A higher turbo-efficiency also follows from a high propeller efficiency, since the ratio between thrust and power increases, see 2.1.6. In order to increase pitch and maintain stable flight, either the propeller angular velocity or diameter has to be decreased. Which of these should be changed depends on the motor, and at what load and angular velocity it has the best efficiency. It should be noted however, that the turbo-efficiency increases with a smaller propeller diameter.

These two strategies might have different effects on the drone performance that need to be taken into account when applying them. Since shifting the efficiency peak by tweaking the blade pitch is a very well tried method, see *variable pitch propellers* [24], this is likely a safe option. However, increasing the propeller pitch might have a negative effect on the take off ability, since a high pitch propeller is likely to stall at low airspeed and advance ratios. The first strategy might be a good option in order to maintain the propulsive efficiency. When deciding which of these methods to apply, the effect on the motor efficiency should also be taken into account. The strategy that maximizes propeller- turbo- and motor efficiency is preferred.

6.1.4 Takeoff Capability

The takeoff capability of the drone can be deemed harsh and limiting because the acceleration takes place under a very short time leading to a high required thrust. Only a handful of propellers managed to match the requirements needed at takeoff. This causes an over-fitting of sorts on the propeller screening which in turn causes propellers to be disregarded early. The propellers that did exceed the thrust limit all have a high pitch, generating more thrust than needed in loiter, where the drone will spend most of its time. This harsh ranking can be linked to the short time in takeoff, as can be seen in table VII. By increasing the takeoff time, it will in turn lower the power consumption, as well as other limiting factors. By lowering the takeoff capability requirements, more propellers will be included after the screening

6.1.5 Error Survey and Data assessment for Propeller Selection

There are some problems with the screening methods which are important to mention. First of all, it is estimated that the propeller will have to run at roughly 9000 rpm and at sprint which is when the propeller runs at its highest. The programs have been running the code at 9000 rpm at sprint, while the measurements from the database span between only 5000 - 7000 rpm. Therefore it is expected that there is some error in the propeller coefficients that have been used to calculate the thrust, power and efficiency at sprint. This is why it is of such importance that these propellers be run at the conditions expected for actual flight, since the computations in MATLAB is susceptible to error. For takeoff and loiter the angular velocities are in the range 5000 - 7000 rpm and therefore these estimations are likely to be more accurate.

Another reason for inaccuracies from the propeller screening is that the measurements from the database might be bad. For example, some propeller data show negative efficiencies, which means that the propeller runs backwards. Other times data points would be repeated over and over again (similar to a flat line), so very few data points were actually useful for the approximations. Sometimes propellers did not pass the screenings, simply because the measurements were bad and the code could not be run properly even if the propeller specifications like diameter and pitch seemed reasonable. It is probable that some propellers that would have worked well for this application were filtered out for that reason. It is also not known how accurate the testing facilities for the database is, which can also contribute to inaccurate approximations.

An additional reason of error could come from the UAV-simfile. First of all the drone is still in prototype stage, and the UAV design is still changing. This means that the simulation data that has been used in the propeller screening could in time become inaccurate and unrepresentative of the final design. It is also a problem that the final weight is currently unknown. A higher drone weight would also mean that the drone needs to produce more lift in order to have balanced flight. More

lift would also induce more drag. This change in lift and drag would in turn change the force equilibrium, meaning that the UAV-simulation data would now be inaccurate, especially if the weight becomes more than the lift data in the simulation file can counteract. Since the propeller calculations use the simulation data to find the minimum required thrust this would make the calculations regarding propeller performance and ranking inaccurate.

6.1.6 Further Propeller Research Suggestions

The results indicate that the propellers available on the UIUC database [18] are a bad match for the drone and mission specified in section 1.3.1. Therefore, there might be an interest to customize the propellers such that they are well fitted for the conditions and constraints set for the UAV. One interesting subject of research would be regarding the pitch of the propellers. For example finding how the pitch can be adjusted in order to fit the propeller better to the mission conditions. Introducing softer, or even removing, the takeoff requirements can allow for more propellers to be considered and studied, since the propellers that did pass the takeoff requirements overproduce thrust in loiter and sprint.

6.2 Motor Selection Process

In this section the motor selection process is concluded with a deeper analysis and concluding arguments. The section also digs deeper into the error survey and further research questions.

6.2.1 Motor Selection

It can be concluded that the motor required to reach the goal of the project tend to be within a specific range of specifications. As mentioned in 4.2.2 some motors were not present on the market and could not be bought and tested in the wind tunnel, which caused a natural narrowing of motors that could not be avoided. Some of the motors that did pass the screening were too big to fit in the testing rig and therefore were not chosen. More information about further research and improvements can be found under section 6.2.3.

6.2.2 Error Survey and Data Conclusion for Motor Selection

An important part of the motor screening were the torque equations used to find the best propeller-motor match. These equations were a conservative estimate of the torque since the actual torque is rather difficult to calculate with the absence of specific data. This leads to inconclusive theoretical estimation of motor torque values. This value is arbitrary value that allows for an educated estimation of the actual torque to be made.

Motor data was scarce and unreliable due to the fact that most of the motors are used by RC-plane enthusiasts. A detailed specification sheet for each of the motors could not be found, hence the values provided had to be accepted in order to move forward with an informative decision about the motors at hand.

It is expected that the values achieved from testing phase will differ significantly from the calculated values. In order to truly determine the most efficient motor, heat maps of the specific motors have to be plotted and analysed. The next section of this project will aim to analyse the efficiency of the motors at different angular velocities and different wind speeds. This will enable the selection of the most effective motor in order to achieve an efficient propulsive system.

6.2.3 Further Motor Research Suggestions

Given the motors used for this project were small scale enthusiast motors, the data regarding the motors and its reliability was questionable. To further improve upon this, finding motors with detailed data sheets provided from a primary source can help provide more reliable data points when screening the motors and less room for errors to take place in addition to less time being wasted. With the given information, it would be deemed most suitable to design and manufacture a motor instead of buying a third-party motor. This could ultimately provide the drone with better options for the propulsive system.

6.3 Rig Redesign Process

The redesign of the testing rig was necessary in order to get accurate results from the sensors. If the original testing rig were to be used in the wind tunnel, there would be wind pushing on the sensors causing inaccurate results. The design process had to be iterated many times since there were no other CAD-files available on the original test rig itself, measurements were taken manually and applying the right tolerances was hard in order to make everything fit when assembling the whole rig.

When first testing the rig in the wind tunnel, several errors surfaced. There were clashes between the airfoils and the sensors which created faulty values when blowing wind onto the rig. To solve this, material had to be removed in the CAD-model from the parts clashing and reprinted, and reassembled which lead to time losses. Also, the motor mounts could not handle the torque created by the motor and propeller when running at high angular velocities which resulted in the rig partially breaking apart. In the end, the original motor mount from the provided testing rig was used even though it was a less aerodynamic shape.

Failure is a common occurrence in a design process and is also needed in order to identify the weak parts in a product. Therefore testing and iterating the design of the rig played a big role in the process of identifying errors with design and tolerances.

The rig was redesigned around the sensors and circuit boards provided from TyTo Robotics which had its limitations. For future research, developing a completely new rig structure using other types sensors and not being dependant on a already existing rig structure could be an option. The consequence of this would be more freedom regarding the design itself, but also better sensors could be used in order to collect more reliable data.

6.4 Wind Tunnel Measurements

A deeper analysis of the different factors involved with the motor and propeller measurements acquired from the wind tunnel testing is concluded in this section.

6.4.1 Theoretical and Practical Test Outcome

Due to all the malfunctions that occurred while testing in the wind tunnel, it can be deduced that the presumed best propeller that was calculated using the propeller database from UIUC does not match when applied in practice, this is also assuming that the database is correct, which it might not be, but it is only used as a reference. However, the mismatching is not necessarily caused by the propeller. The propulsive system could not utilize enough current at high wind speeds to reach the required angular velocities, this led to our results for that specific propeller tested being inconclusive.

6.4.2 Error Survey Wind Tunnel Measurements

While testing the motor and propeller combination in the wind tunnel, there were many factors that affected the end result which are discussed here.

When calculating C_P, there are many parameters which could have affected the result. The hub used to attach the propellers to the motor differed to the one used in the database. The result of this is a displacement of the blade pitch making the angle of attack differ from the optimal one and a propeller diameter that might not be the same as in the UIUC database tests. Fluctuations when measuring the angular velocity also occurred which was contributing factor to uncertainties in determining C_P and motor efficiencies. The built-in rpm-sensor in the testing rig was used which was not accurate enough. To try and mitigate this the mean value of the angular velocities across ≈100 data points was used which gave more reliable values but did not entirely salve the issue. The measured errors in angular velocity could reach upwards of 10%, which has an adverse negative effect as a large standard deviation will give highly inaccurate values across all data points. This was reflected in the standard deviation heat maps in Fig. 20. An example of error in efficiency can be easily calculated with (28) on a single data point example in XV
The efficiency can vary a significant amount when using the in built rpm sensor and this has to be taken into consideration when using the motor efficiency heat map in places where the standard deviation is large. For further research, an optical angular velocity sensor could be used in order to get stable and accurate measurements.

TABLE XV
ERROR VARIATION WITH A STANDARD DEVIATION OF 400 RPM FOR A SINGLE MOTOR DATA POINT

RPM	Tq	P_{el}	η
7400	0.1352	133.75	0.783
7000	0.1352	133.75	0.741
6600	0.1352	133.75	0.677

In order to achieve higher angular velocities, the testing rig utilized current close to the power supply's limit, otherwise known as the "Burst Current" at 25 A. The current can only be "bursted" for a short while before "Over Current Protection" turns off the power supply as a protective measure and as a result testing in 35 m/s could no be carried out since the power supply used in testing could not provide adequate current necessary for the motor to reach the higher angular velocities.

There were also a risk of damaging the rig leading to further delays in the testing process. Damaging the rig caused ESC overheating and prevented it from providing the required angular velocity and therefore providing unreliable rpm-readings. In addition to that, the efficiency gradually decreased when reaching higher temperatures. Therefore the rig had to be disassembled and cooled down between each test. Since one of the aims was to run a complete mission, this was a non desirable adverse effect. For further research, ventilation canals for cooling must be implemented in the design in order to cool the system and to be able to run longer tests.

The 11x10 propeller was subject to a combination of all of the above errors, but mostly the measurement of the angular velocities was inconsistent. At high angular velocities, the rpm-probe measured values with high variance, and therefore the data obtained after the post processing was very uncertain. The final data from the 11x10 was inconclusive and was not following the trend expected for any of the propeller coefficients. Therefore, it was not presented in the report. When the 11x8.5 propeller was tested in the wind tunnel, it was observed that there were a lot of noise and oscillation in the rig making the sensors deviate. This likely has had a significant effect on the measurements of torque and angular velocities.

6.5 Fulfillment of the Purpose

The main purpose of this project is to find the propulsive components (such as propellers and motors), available on the market best suited for the drone mission specified in 1.3.1. The objective is to optimize the drone propulsive performance by minimizing the power- and energy consumption. The purpose can be considered as mostly fulfilled since a preliminary recommendation for a combination of a propeller and a motor has been presented. However, due to several flaws in the final testing

phase presented in sections 6.1.5, 6.2.2, and 6.4.2, all of the propulsive components could not be tested, and therefore the available propeller-motor combination options were limited. As a result, the data necessary to make a final recommendation for a propeller- and motor combination was insufficient. All of the secondary objectives stated in section 1.1 were fulfilled and contributed to the main purpose, except the goal of identifying each propulsive components' energy consumption as well as their energy consumption for an entire mission. The reason for this not being fulfilled is presented in 6.4.2.

Bibliography

[1] R. Y. Myose and R. J. Strohl, "Uninhabited aerial vehicle (UAV)," *AccessScience*, 2020. [Online]. Available: https://www.accessscience.com/content/uninhabited-aerial-vehicle-uav/205300, (accessed: 09-03-2022).

[2] S. Hedvall, *Spaningsflygplan*. [Online]. Available: https://digitaltmuseum.se/021026436584/spaningsflygplan, (accessed: 15-02-2022).

[3] G. Alley-Young, "Drone (unmanned aerial vehicle).," *Salem Press Encyclopedia*, 2020. [Online]. Available: https://search.ebscohost.com/login.aspx?direct=true&db=ers&AN=87321880&site=eds-live&scope=site&authtype=guest&custid=s3911979&groupid=main&profile=eds, (accessed: 09-03-2022).

[4] NASA, *Blended wing body – a potential new aircraft design*. [Online]. Available: https://www.nasa.gov/centers/langley/news/factsheets/FS-2003-11-81-LaRC.html, (accessed: 15-02-2022).

[5] NASA via Rawpixel, *The X-48B Blended Wing Body research aircraft*. [Online]. Available: https://www.flickr.com/photos/vintage_illustration/46363519941, (accessed: 15-02-2022).

[6] USA today, "15 commercial products invented by the military include GPS, duct tape and Silly Putty," *USA today*, [Online]. Available: https://eu.usatoday.com/story/money/2019/05/16/15-commercial-products-invented-by-the-military/39465501/.

[7] Business Insider, "Drone technology uses and applications for commercial, industrial and military drones in 2021 and the future," *Insider*, 2021. [Online]. Available: https://www.businessinsider.com/drone-technology-uses-applications?r=US&IR=T, (accessed: 15-02-2022).

[8] E. Torenbeek and H. Wittenberg, *Flight Physics. [electronic resource] : Essentials of Aeronautical Disciplines and Technology, with Historical Notes*. Springer Netherlands, 2009, pp. 236–249, ISBN: 9781402086649. [Online]. Available: https://search.ebscohost.com/login.aspx?direct=true&db=cat07472a&AN=clec.SPRINGERLINK9781402086649&site=eds-live&scope=site&authtype=guest&custid=s3911979&groupid=main&profile=eds.

[9] P. M. Sforza, *Theory of Aerospace Propulsion.* Ser. Aerospace Engineering Ser. Elsevier Science Technology, 2016, p. 520, ISBN: 9780128096017. [Online]. Available: https://search.ebscohost.com/login.aspx?direct=true&db=cat07472a&AN=clec.EBC5754527&site=eds-live&scope=site&authtype=guest&custid=s3911979&groupid=main&profile=eds.

[10] MIT, *Performance of propellers.* [Online]. Available: https://web.mit.edu/16.unified/www/FALL/thermodynamics/notes/node86.html, (accessed: 24-04-2022).

[11] Helicel, *The propulsive efficiency of the screw propeller efficiency.* [Online]. Available: https://www.heliciel.com/en/helice/calcul-helice-aile/rendement-helice-propulsive.htm#equation, (accessed 08-05-2022).

[12] A. Lind, "Aerodynamic Simulations of an Innovative High Speed Propeller," Ph.D. dissertation, Chalmers University of Technology, 2013.

[13] C. Xisto et. al, "Technologies and innovations for a future sustainable hydrogen economy," p. 29, 2021.

[14] Northeastern University, *Electromagnets.* [Online]. Available: https://ece.northeastern.edu/fac-ece/nian/mom/electromagnets.html, (accessed: 21-02-2022.

[15] P. Millet, *Brushless Vs Brushed DC Motors: When and Why to Choose One Over the Other.* [Online]. Available: https://www.monolithicpower.com/en/brushless-vs-brushed-dc-motors, (accessed: 21-02-2022).

[16] Tyto Robotics, *All derived efficiencies explanation.* [Online]. Available: https://www.tytorobotics.com/blogs/general-knowledge/all-derived-efficiency-explanation, (accessed: 24-02-2022).

[17] M. Drela, *First-Order DC Electric Motor Model.* [Online]. Available: https://web.mit.edu/drela/Public/web/qprop/motor1_theory.pdf, (accessed: 21-02-2022).

[18] J. B. Brandt et al., *UIUC Propeller Data Site.* [Online]. Available: https://m-selig.ae.illinois.edu/props/propDB.html, (accessed: 21-02-2022).

[19] Unmanned System Technology, *Electronic Speed Controllers (ESC).* [Online]. Available: https://www.unmannedsystemstechnology.com/expo/electronic-speed-controllers-esc/, (accessed: 24-04-2022).

[20] F. White, *Fluid Mechanics.* McGraw-Hill Professional, The importance of streamlining in reducing drag, 2015, p. 456, ISBN: 9780073398273. [Online]. Available: https://search.ebscohost.com/login.aspx?direct=true&db=cat07470a&AN=clc.db6990df.c39c.4154.9493.0703259cd521&site=eds-live&scope=site.

[21] C. J. Peel, "Aircraft testing," *AccessScience*, 2019. [Online]. Available: https://www-accessscience-com.proxy.lib.chalmers.se/content/aircraft-testing/019400, (accessed: 09-03-2022).

[22] helveciotf, *EMAX Brushless Motor Technical Data.* [Online]. Available: https://www.scribd.com/doc/316240006/EMAX-brushless-motor-technical-data-pdf, (accessed: 18-02-2022).

[23] EMAX, *GT & XA XT Series motors*. [Online]. Available: https://emaxmodel.com/collections/gt-xa-xt-series-motors, (accessed: 18-02-2022).

[24] H. V. Borst, "Propeller (aircraft)," *AccessScience*, 2020. [Online]. Available: https://www-accessscience-com.proxy.lib.chalmers.se/content/propeller-aircraft/548600, (accessed: 11-05-2022).

A

Propeller Data Tables for Top 4 Best Performing Propellers

TABLE XVI

AERONAUT CARBON ELECTRIC 11X10 AT STABLE FLIGHT FOR DIFFERENT WEIGHTS AND VELOCITIES

Weight [kg]		**2.0**			**2.5**			**3.0**			**3.5**	
Time in mode [min]	**0.5**	**40**	**20**	**0.5**	**40**	**20**	**0.5**	**40**	**20**	**0.5**	**40**	**20**
Airspeed [m/s]	**15**	**22**	**35**	**15**	**22**	**35**	**15**	**22**	**35**	**15**	**22**	**35**
UAV AoA [deg]	6.85	2.38	0.11	9.31	3.32	0.48	12.58	4.28	0.85	17.16	5.25	1.22
UAV D [N]	1.14	1.37	2.91	1.62	1.53	2.97	2.47	1.73	3.04	3.91	1.97	3.12
Minimum required T [N]	1.14	1.37	2.91	1.59	1.53	2.97	2.57	1.73	3.04	5.98	1.96	3.12
T [N]	1.91	1.43	2.97	1.91	1.55	2.97	2.59	1.73	3.07	6.01	2.01	3.18
C_T	0.06	0.03	0.02	0.06	0.03	0.02	0.07	0.03	0.02	0.09	0.04	0.03
C_P	0.06	0.04	0.04	0.06	0.04	0.04	0.07	0.05	0.04	0.07	0.05	0.04
P [W]	37.83	49.30	172.82	37.83	52.39	172.82	50.52	56.90	176.94	119.43	64.15	181.02
$\eta_{propeller}$	0.76	0.65	0.64	0.76	0.66	0.64	0.77	0.68	0.64	0.75	0.69	0.64
$\eta_{propulsive}$	0.95	0.98	0.98	0.95	0.98	0.98	0.93	0.98	0.98	0.87	0.97	0.98
η_{turbo}	0.82	0.78	0.77	0.83	0.78	0.77	0.85	0.79	0.77	0.88	0.80	0.77
n [rpm]	4000	4956	7770	4000	4992	7770	4307	5046	7788	5533	5136	7806
J	0.81	0.95	0.97	0.81	0.95	0.97	0.75	0.94	0.97	0.58	0.92	0.96
Time spent in mode [min]	0.5	40	20	0.5	40	20	0.5	40	20	0.5	40	20
Total Energy Consum. [kJ]		326.8			334.3			350.4			374.8	

TABLE XVII
Aeronaut Carbon Electric 11x8 at stable flight for different weights and velocities

Weight [kg]		**2.0**			**2.5**			**3.0**			**3.5**	
Time in mode [min]	**0.5**	**40**	**20**	**0.5**	**40**	**20**	**0.5**	**40**	**20**	**0.5**	**40**	**20**
Airspeed [m/s]	**15**	**22**	**35**	**15**	**22**	**35**	**15**	**22**	**35**	**15**	**22**	**35**
UAV AoA [deg]	6.85	2.38	0.11	9.31	3.32	0.48	12.58	4.28	0.85	17.16	5.25	1.22
UAV D [N]	1.14	1.37	2.91	1.62	1.53	2.97	2.47	1.73	3.04	3.91	1.97	3.12
Minimum required T [N]	1.14	1.37	2.91	1.59	1.53	2.97	2.57	1.73	3.04	5.98	1.96	3.12
T [N]	1.15	1.40	2.93	1.59	1.55	3.00	2.58	1.74	3.07	5.99	1.97	3.14
C_T	0.03	0.02	0.02	0.04	0.02	0.02	0.05	0.02	0.02	0.07	0.02	0.02
C_P	0.03	0.02	0.02	0.03	0.03	0.02	0.04	0.03	0.02	0.05	0.03	0.02
P [W]	24.31	50.91	181.97	32.02	54.18	184.56	50.19	58.61	187.17	120.20	64.16	189.80
$\eta_{propeller}$	0.71	0.61	0.56	0.75	0.63	0.57	0.77	0.65	0.57	0.75	0.68	0.58
$\eta_{propulsive}$	0.97	0.98	0.98	0.96	0.98	0.98	0.93	0.98	0.98	0.87	0.97	0.98
η_{turbo}	0.65	0.32	0.13	0.74	0.40	0.15	0.81	0.48	0.17	0.86	0.55	0.19
n [rpm]	4379	6002	9393	4613	6056	9411	5082	6128	9429	6399	6218.437	9446.894
J	0.74	0.79	0.80	0.70	0.78	0.80	0.63	0.77	0.80	0.50	0.76	0.80
Time spent in mode [min]	0.5	40	20	0.5	40	20	0.5	40	20	0.5	40	20
Total enegy consum [kJ]		341.3			352.5			366.8			385.3	

TABLE XVIII

Aeronaut Carbon Electric 10x8 at stable flight for different weights and velocities

Weight [kg]		**2.0**			**2.5**			**3.0**			**3.5**	
Time in mode [min]	**0.5**	**40**	**20**	**0.5**	**40**	**20**	**0.5**	**40**	**20**	**0.5**	**40**	**20**
Airspeed [m/s]	**15**	**22**	**35**	**15**	**22**	**35**	**15**	**22**	**35**	**15**	**22**	**35**
UAV AoA [deg]	6.85	2.38	0.11	9.31	3.32	0.48	12.58	4.28	0.85	17.16	5.25	1.22
UAV D [N]	1.14	1.37	2.91	1.62	1.53	2.97	2.47	1.73	3.04	3.91	1.97	3.12
Minimum required T [N]	1.14	1.37	2.91	1.59	1.53	2.97	2.57	1.73	3.04	5.98	1.96	3.12
T [N]	1.16	1.41	2.96	1.61	1.55	3.02	2.60	1.74	3.07	6.02	2.00	3.13
C_T	0.04	0.03	0.02	0.05	0.03	0.02	0.06	0.03	0.02	0.09	0.03	0.02
C_P	0.04	0.04	0.03	0.05	0.04	0.03	0.05	0.04	0.03	0.06	0.04	0.03
P [W]	24.26	49.40	175.73	32.40	52.83	177.86	51.14	57.41	179.98	125.88	63.92	182.10
$\eta_{propeller}$	0.71	0.63	0.59	0.75	0.64	0.59	0.76	0.66	0.60	0.72	0.69	0.60
$\eta_{propulsive}$	0.96	0.98	0.98	0.95	0.98	0.98	0.92	0.97	0.98	0.85	0.97	0.98
η_{turbo}	0.74	0.64	0.60	0.79	0.66	0.61	0.83	0.68	0.61	0.85	0.71	0.61
n [rpm]	4559	6164	9609	4848	6236	9627	5407	6327	9645	6976	6453	9663
J	0.78	0.84	0.86	0.73	0.83	0.86	0.66	0.82	0.86	0.51	0.81	0.86
Time spent in mode [min]	0.5	40	20	0.5	40	20	0.5	40	20	0.5	40	20
Total enegy consum [kJ]		330.2			341.2			355.3			375.7	

TABLE XIX

APC Thin Electric Electric 11x8.5 at stable flight for different weights and velocities

Weight [kg]		**2.0**			**2.5**			**3.0**			**3.5**	
Time in mode [min]	**0.5**	**40**	**20**	**0.5**	**40**	**20**	**0.5**	**40**	**20**	**0.5**	**40**	**20**
Airspeed [m/s]	**15**	**22**	**35**	**15**	**22**	**35**	**15**	**22**	**35**	**15**	**22**	**35**
UAV AoA [deg]	6.85	2.38	0.11	9.31	3.32	0.48	12.58	4.28	0.85	17.16	5.25	1.22
UAV D [N]	1.14	1.37	2.91	1.62	1.53	2.97	2.47	1.73	3.04	3.91	1.97	3.12
Minmum required T [N]	1.14	1.37	2.91	1.59	1.53	2.97	2.57	1.73	3.04	5.98	1.96	3.12
T [N]	1.15	1.39	2.95	1.60	1.57	3.02	2.60	1.75	3.08	6.00	1.98	3.14
C_T	0.03	0.02	0.02	0.04	0.02	0.02	0.05	0.02	0.02	0.08	0.02	0.02
C_P	0.03	0.02	0.02	0.04	0.03	0.02	0.04	0.03	0.02	0.05	0.03	0.02
P [W]	25.13	49.65	177.21	33.83	54.35	179.77	53.28	59.35	182.36	125.79	65.54	184.98
$\eta_{propeller}$	0.69	0.61	0.58	0.71	0.63	0.59	0.73	0.65	0.59	0.72	0.66	0.59
$\eta_{propulsive}$	0.97	0.98	0.98	0.96	0.98	0.98	0.93	0.98	0.98	0.87	0.97	0.98
η_{turbo}	0.66	0.45	0.34	0.72	0.51	0.35	0.78	0.55	0.36	0.82	0.59	0.37
n [rpm]	4361	5966	9339	4595	6038	9357	4992	6110	9375	6200	6200	9393
J	0.74	0.79	0.80	0.70	0.78	0.80	0.65	0.77	0.80	0.52	0.76	0.80
Time spent in mode [min]	0.5	40	20	0.5	40	20	0.5	40	20	0.5	40	20
Total Energy Consum. [kJ]		332.6			347.2			362.9			383.0	

B

Motor-Propeller Matching Process

This shows the method used to screen and sort the motors in a step-by-step manner.

No load rpm per volt (K_v): Given in [rpm/V]
Maximum power ($P_{m,max}$): Given in [W]
Maximum current ($i_{m,max}$): Given in [A]
Angular velocity for takeoff (Ω_t): Calculated in propeller screening in [rpm]
Angular velocity for loiter (Ω_l): Calculated in propeller screening in [rpm]
Angular velocity for sprint (Ω_s): Calculated in propeller screening in [rpm]
Power required in takeoff (P_t): Calculated in propeller screening in [W]
Power required in loiter (P_l): Calculated in propeller screening in [W]
Power required in sprint (P_s): Calculated in propeller screening in [W]

Using the above values, calculations can be made to find
Voltage required in takeoff, loiter, and sprint respectively:

$$V_{t,l,s} = \frac{\Omega_{t,l,s}}{K_v}$$

Current required in takeoff, loiter, and sprint respectively can then be calculated as:

$$i_{t,l,s} = \frac{V_{t,l,s}}{P_{t,l,s}}$$

If the maximum power was smaller than the required power in takeoff, loiter, or sprint, the motor passed the first screening. If the power required only exceeded in takeoff it was deemed safe, and passed to the second screening. All other motors were disregarded.

These steps were then performed for the current required:
Calculated propeller torque (Q_{prop}): Calculated in this method in [Nm]
Calculated motor torque for takeoff ($Q_{m,t}$): Calculated in this method in [Nm]
Calculated motor torque for loiter ($Q_{m,l}$): Calculated in this method in [Nm]
Calculated motor torque for sprint ($Q_{m,s}$): Calculated in this method in [Nm]

In the second part of the screening the motors were ranked based on the seven criteria, of which the *motor-propeller torque difference percentage* was one of them. To find a point of reference, a pre-test was made, where one data point prior to the data collection stage was used in order to gather some knowledge about the values to

expect. To calculate the *motor-propeller torque difference percentage* the following method was used:

Recorded torque from pre-test: Q_{rec}
Recorded current from pre-test: i_{rec}

Using i_{rec} and i_0, the calculated torque can be found for a specific motor. This is then used to determine the "margin of safety" these equations use.

$$Motor - Propeller\ Torque\ Difference\ Percentage = \frac{Q_{rec} - \frac{i - i_0}{K_v}}{Q_{rec}}$$

In this case this proved to be around 35%. This difference percentage was then applied to all other motors and used to determine which motors would not be suitable from a torque-matching perspective. If the motor-propeller torque difference percentage exceeded the calculated percentage, the motors were discarded. This was compared on both loiter and sprint values. It is important to note that since not all motors underwent a pre-test, Q_{rec} is substituted for the desired torque or in other words Q_{prop}. This creates the following statement:

$$\frac{Q_{prop} - \frac{i - i_0}{K_v}}{Q_{prop}} \leq 35\%$$

The motors that passed the two screenings were then acquired based on the seven criteria mentioned in 3.2.2. The motor with the largest score should then theoretically be the best motor for the job.

C

Wind Tunnel Test Measurements

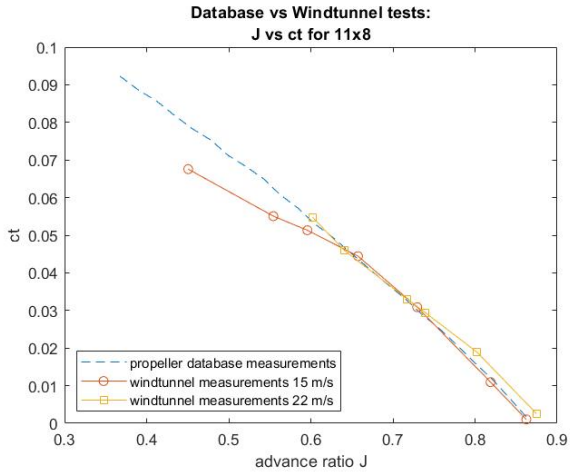

(a) Thrust coefficient derived from wind tunnel measurements for 11x8 propeller

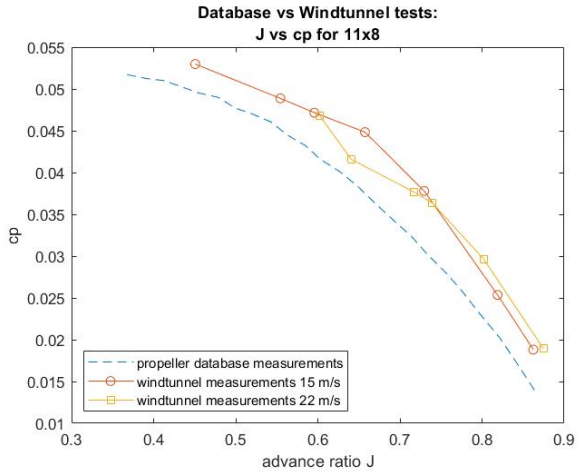

(b) Power coefficient derived from wind tunnel measurements for 11x8 propeller

Fig. 23. Derived propeller coefficients from wind tunnel measurements.

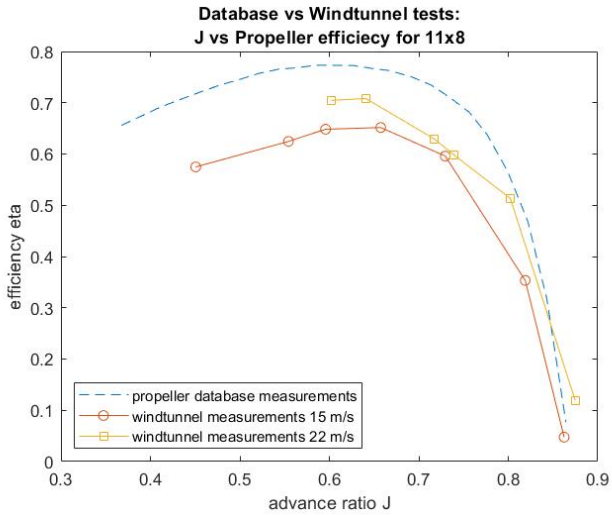

Fig. 24. Derived advance ratio plotted against efficiency for the 11x8 propeller.

TABLE XX
WIND TUNNEL MEASUREMENTS FOR AERONAUT CARBON ELECTRIC 11X8 AT WIND SPEED 15 M/S

Measured V [m/s]	**Measured n [rpm]**	$\boldsymbol{Q}$ **[N/m]**	$\boldsymbol{T}$ **[N]**	$\boldsymbol{\eta_m}$
15.05	3799	0.023	0.029	0.548
15.08	4009	0.034	0.338	0.583
15.10	4506	0.065	1.204	0.621
15.12	5007	0.095	2.141	0.664
15.15	5536	0.122	3.022	0.692
15.20	5970	0.147	3.771	0.734
15.22	7353	0.241	7.020	0.808
[°C]	23.95			
ρ [kg/m^3]	1.199			

TABLE XXI
DERIVED COEFFICIENTS FOR CARBON ELECTRIC 11X8 FROM MEASUREMENTS AT WIND SPEED 15 M/S

$\boldsymbol{J}$	$\boldsymbol{C_T}$	$\boldsymbol{C_Q}$	$\boldsymbol{C_P}$	$\boldsymbol{P}$ **[W]**	$\boldsymbol{\eta_{Propeller}}$
0.862	0.001	0.003	0.019	9.11	0.048
0.819	0.011	0.004	0.025	14.42	0.353
0.730	0.031	0.006	0.038	30.52	0.596
0.657	0.044	0.007	0.045	49.66	0.652
0.596	0.051	0.008	0.047	70.62	0.648
0.554	0.055	0.008	0.049	91.78	0.625
0.451	0.068	0.008	0.053	185.89	0.575

TABLE XXII
WIND TUNNEL MEASUREMENTS FOR AERONAUT CARBON ELECTRIC 11X8 AT WIND SPEED 22 M/S

Measured V [m/s]	**Measured n [rpm]**	$\boldsymbol{Q}$ **[N/m]**	$\boldsymbol{T}$ **[N]**	$\boldsymbol{\eta_m}$
22.1	5500	0.048	0.15	0.572
22.1	5997	0.090	1.31	0.647
22.1	6505	0.130	2.39	0.676
22.1	6708	0.143	2.86	0.674
22.1	7511	0.198	4.99	0.699
22.1	7989	0.252	6.72	0.722
T [°C]	23.95			
ρ [kg/m^3]	1.203			

TABLE XXIII
DERIVED COEFFICIENTS FOR CARBON ELECTRIC 11X8 FROM MEASUREMENTS AT WIND SPEED 22 M/S

$\boldsymbol{J}$	$\boldsymbol{C_T}$	$\boldsymbol{C_Q}$	$\boldsymbol{C_P}$	$\boldsymbol{P}$ **[W]**	$\boldsymbol{\eta_{Propeller}}$
0.875	0.003	0.003	0.019	27.82	0.119
0.802	0.019	0.005	0.030	56.40	0.513
0.740	0.029	0.006	0.036	88.38	0.598
0.717	0.033	0.006	0.038	100.40	0.630
0.641	0.046	0.007	0.042	155.68	0.708
0.602	0.055	0.007	0.047	210.77	0.705

(a) Power coefficient

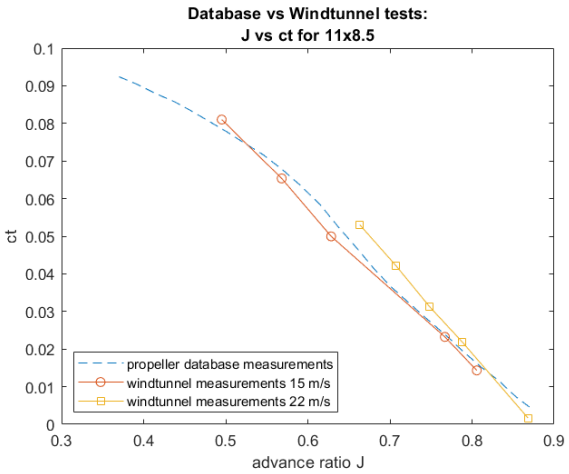

(b) Thrust coefficient

Fig. 25. Power and Thrust coefficient plotted against advance ratio for APC Thin Electric 11x8.5 Propeller. Measurements from database and measurements from wind tunnel included in the figure.

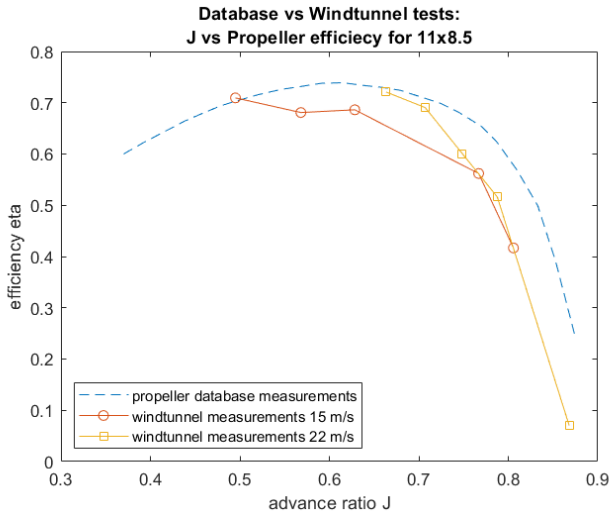

Fig. 26. Derived advance ratio plotted against efficiency for the 11x8.5 propeller.

TABLE XXIV
WIND TUNNEL MEASUREMENTS FOR APC THIN ELECTRIC 11X8.5 AT WIND SPEED 15 M/S

Measured V [m/s]	**Measured n [rpm]**	$\boldsymbol{Q}$ **[N/m]**	$\boldsymbol{T}$ **[N]**	$\boldsymbol{\eta_m}$
15.03	6520	0.217	6.990	0.730
15.08	5700	0.160	4.310	0.730
15.10	5160	0.110	2.700	0.690
15.07	4220	0.051	0.840	0.630
15.01	4000	0.040	0.470	0.600
T [°C]	23.95			
ρ [kg/m^3]	1.199			

TABLE XXV
DERIVED COEFFICIENTS FOR APC THIN ELECTRIC 11X8.5 FROM MEASUREMENTS AT WIND SPEED 15 M/S

$\boldsymbol{J}$	$\boldsymbol{C_T}$	$\boldsymbol{C_Q}$	$\boldsymbol{C_P}$	$\boldsymbol{P}$**[W]**	$\boldsymbol{\eta_{propeller}}$
0.500	0.080	0.009	0.060	148.09	0.710
0.570	0.065	0.009	0.060	95.46	0.680
0.630	0.050	0.007	0.050	59.41	0.690
0.770	0.020	0.005	0.030	22.53	0.560
0.810	0.010	0.004	0.030	16.75	0.420

TABLE XXVI
WIND TUNNEL MEASUREMENTS FOR APC THIN ELECTRIC 11X8.5 AT WIND SPEED 22 M/S

Measured V [m/s]	**Measured n [rpm]**	$\boldsymbol{Q}$ **[N/m]**	$\boldsymbol{T}$ **[N]**	$\boldsymbol{\eta_m}$
21.96	7110	0.221	5.400	0.850
22.06	6700	0.174	3.820	0.780
21.96	6300	0.138	2.490	0.815
22.01	6000	0.108	1.590	0.795
21.95	5430	0.055	0.100	0.730
T [°C]	24.26			
ρ [kg/m^3]	1.197			

TABLE XXVII
DERIVED COEFFICIENTS FOR APC THIN ELECTRIC 11X8.5 FROM MEASUREMENTS AT WIND SPEED 22 M/S

$\boldsymbol{J}$	$\boldsymbol{C_T}$	$\boldsymbol{C_Q}$	$\boldsymbol{C_P}$	$\boldsymbol{P}$ **[W]**	$\boldsymbol{\eta_{Propeller}}$
0.660	0.053	0.008	0.050	164.46	0.720
0.710	0.042	0.007	0.040	122.02	0.690
0.758	0.030	0.006	0.040	91.00	0.600
0.790	0.020	0.005	0.030	67.82	0.520
0.870	0.002	0.003	0.020	31.26	0.070

DEPARTMENT OF MECHANICS AND MARITIME SCIENCES
CHALMERS UNIVERSITY OF TECHNOLOGY
Gothenburg, Sweden
www.chalmers.se

CHALMERS